Applied Geochemistry 96 (2018) 287–301

Contents lists available at ScienceDirect

Applied Geochemistry

journal homepage: www.elsevier.com/locate/apgeochem

Linking serpentinization, hyperalkaline mineral waters and abiotic methane production in continental peridotites: an integrated hydrogeological-biogeochemical model from the Cabeço de Vide CH_4-rich aquifer (Portugal)

J.M. Marques[a,*], G. Etiope[b], M.O. Neves[a], P.M. Carreira[c], C. Rocha[a], S.D. Vance[d], L. Christensen[d], A.Z. Miller[e], S. Suzuki[f]

[a] Centro de Recursos Naturais e Ambiente (CERENA), Instituto Superior Técnico, Universidade de Lisboa, Av. Rovisco Pais, 1049-001, Lisboa, Portugal
[b] Istituto Nazionale di Geofisica e Vulcanologia, Sezione Roma 2, Via V. Murata 605 00143 Roma, Italy and Faculty of Environmental Science and Engineering, Babes-Bolyai University, Cluj-Napoca, Romania
[c] Centro de Ciências e Tecnologias Nucleares (C^2TN/IST), Instituto Superior Técnico, Universidade de Lisboa, Estrada Nacional 10, ao km 139,7, 2695-066, Bobadela, LRS, Portugal
[d] Jet Propulsion Laboratory, California Institute of Technology, MS 321-560 4800 Oak Grove Dr. Pasadena, CA, 91109, USA
[e] Instituto de Recursos Naturales y Agrobiología de Sevilla (IRNAS-CSIC), Av. Reina Mercedes 10, 41012, Sevilla, Spain
[f] Kochi Institute for Core Sample Research (JAMSTEC), 200 Monobe Otsu, Nankoku, Kochi, 783-8502, Japan

ARTICLE INFO

Editorial handling by Dr M Liotta

Keywords:
Hyperalkaline mineral waters
Ultramafic rocks
Serpentinization
Abiotic methane
Portugal

ABSTRACT

Continental active serpentinization of ultramafic rocks is today recognized as a key process triggering a sequence of phenomena involving the passage from inorganic, to organic and metabolic reactions. These may have a role in the origin of life, and may explain the occurrence of abiotic hydrocarbons on Earth and other planets. Production of hyperalkaline waters and abiotic methane (CH_4) are two critical steps in this sequence. They were described independently by specific hydrogeological and geochemical models. Here, we update and combine these models into a unified scheme using and integrating geological, hydrogeological, hydrogeochemical, gas-geochemical and microbial analyses acquired from 2002 to 2014 in the Cabeço de Vide (CdV) study site, Portugal. The hyperalkaline (pH > 10.5), Na-Cl/Ca-OH mineral water of CdV evolve from groundwater-peridotite interaction (serpentinization) generating hydrogen (H_2), which, according to multiple theoretical, laboratory and field evidence, likely reacted with CO_2 within metal- (catalyst) rich rocks, abiotically producing CH_4 (up to 1.2 mg/L; -24.4‰ < δ^{13}C-CH_4 < -14.0‰ and -285‰ < δ^2H-CH_4 < -218‰). The hyperalkaline water hosts hydrogen oxidizing bacteria "*Serpentinomonas*", which may explain the paucity of H_2 observed in the dissolved gas. The CdV gas-rich mineral waters ascend along a fault at the boundary of the peridotite intrusion. Temporal changes of pH and CH_4 concentration result from episodic mixing with shallower Mg-HCO_3-type waters. Soil-gas analyses show that methane migrates to the surface along the fault, also independently from the water emergences, consistently with non-aqueous abiotic CH_4 production. Our integrated model is generally compatible with observations from other gas-bearing continental serpentinization sites.

1. Introduction

Over the last decades, serpentinization of ultramafic rocks (peridotites) has been the subject of numerous studies, due to its potential for providing energy sources, such as hydrogen (H_2) and methane (CH_4), for microbial life (e.g., Holm et al., 2006; Russell et al., 2010; Schrenk et al., 2013). By converting energy into biomass, specialised microorganisms have the capability to support full biological communities based on chemical energy rather than photosynthesis. These might be modern analogs of ancient communities that existed on early Earth and on other planetary bodies, such as Mars and the icy ocean worlds Europa, Enceladus, and Titan (e.g., Schulte et al., 2006; Vance et al., 2007, 2016; Russell et al., 2014; Oehler and Etiope, 2017).

Abiotic CH_4, produced by reacting H_2 with CO_2 (Fischer-Tropsch Type or Sabatier reaction; Etiope and Sherwood Lollar, 2013) may, then (a) migrate into conventional (sedimentary) gas-oil systems adjacent to

* Corresponding author.
E-mail addresses: jose.marques@tecnico.ulisboa.pt (J.M. Marques), giuseppe.etiope@ingv.it (G. Etiope), carreira@ctn.tecnico.ulisboa.pt (P.M. Carreira), Steven.D.Vance@jpl.nasa.gov (S.D. Vance), anamiller@irnas.csic.es (A.Z. Miller), sisuzuki@jamstec.go.jp (S. Suzuki).

https://doi.org/10.1016/j.apgeochem.2018.07.011
Received 20 May 2018; Received in revised form 11 July 2018; Accepted 18 July 2018
Available online 20 July 2018
0883-2927/

the peridotite massifs, mixing with biotic (microbial or thermogenic) gas and altering its isotopic character (e.g., Etiope and Schoell, 2014; Etiope et al., 2015), or (b) migrate to the surface and enter the atmosphere as a natural source of greenhouse gas (e.g., Etiope, 2015; Etiope et al., 2017). In addition to a few cases of deep submarine serpentinization sites, such as Lost City in the Atlantic Ocean (Proskurowski et al., 2008; Schrenk et al., 2013), the surface outflow of dominantly abiotic hydrocarbons has been discovered on continents in at least 17 countries (Etiope et al., 2017). In these continental sites gas is issuing from seeps or water springs along faults in ultramafic rocks, belonging to ophiolites, peridotite massifs or igneous intrusions, with evidence of present-day serpentinization driven by meteoric water (e.g., Cipolli et al., 2004; Marques et al., 2008; Morrill et al., 2013; Monnin et al., 2014; Sanchez-Murillo et al., 2014; Suda et al., 2014; Etiope at al. 2017). Methane occurs systematically in all hyperalkaline waters, and has diagnostic combinations of carbon ($^{12}C/^{13}C$) and hydrogen ($^{1}H/^{2}H$) isotope compositions distinct from (only partially overlapping) thermogenic isotopic signature (Etiope and Sherwood Lollar, 2013; Etiope et al., 2017). Hydrogeological/hydrogeochemical models have been proposed to explain the origin of the hyperalkaline waters (e.g., Barnes et al., 1967, 1972; Barnes and O'Neil, 1969; Cipolli et al., 2004; Marques et al., 2008) and gas-geochemical models have been considered for explaining the origin of methane (e.g., Etiope, 2017a; Etiope et al., 2017, 2018).

Here, we combine the two model types using published (Marques et al., 2008; Etiope et al., 2013b) and new data (acquired in 2012, 2013 and 2014) regarding the continental serpentinization site of Cabeço de Vide (CdV), within the Alter-do-Chão pluton (central Portugal). CdV is characterized by the presence of a hyperalkaline (pH > 10) mineral aquifer intercepted by two boreholes (named AC3 and AC5) that bring the water to a therapeutic spa. One mineral spring (named Ermida), three normal springs (named Dos Amores, Borbologão and Sto. António), and a shallow borehole (named Maria Rita) additionally release water with variable chemistry and gas content. Geochemical analyses of these systems, including physico-chemical and isotopic data, have been combined with microbial analyses, methane detection in soil gases, and detailed geological mapping, to develop a unified model explaining the origin and occurrence of the different fluids.

2. Geological setting and methodology

2.1. Geological setting and description of fluid sampling sites

The study region is situated in the Ossa Morena Zone (OMZ) of the Iberian Hercynian belt. The OMZ represents the complex evolution of a continental margin during the Late Paleozoic, associated to the convergence and collision of two large continental masses, Gondwana and Laurasia (Dallmeyer and Quesada, 1992). The OMZ includes an Upper Proterozoic basement showing inliers of high-pressure metamorphic rocks, and a Paleozoic series including bimodal volcanics of a typical intracontinental rift character (Mata and Munhá, 1985; Fonseca and Ribeiro, 1993).

The CdV hyperalkaline mineral water aquifer is located in the Alter-do-Chão pluton, a ring-like intrusion with NW-SE elongated shape, following the Variscan orientation, where the Lower Cambrian carbonate sequence was metamorphosed by the local mafic and ultramafic intrusions (Gonçalves, 1973; Marques et al., 2008). This pluton has been faced as a cumulate-type structure of Ordovician age (Costa et al., 1993). Mafic rocks outcropping in the surroundings the ultramafic core (comprising dunites, serpentinized dunites to serpentinites and peridotites) are mostly coarse-to fine-grained gabbros with Ca-plagioclase, Ti-clinopyroxene, olivine and some Al-hornblende (Costa et al., 1993). Most commonly, the serpentinized ultramafic rocks contain serpentine minerals (lizardite, antigorite and chrysotile), magnetite and residual chromite, plus brucite and carbonates (Fig. 1).

Other geological formations, including Precambrian metamorphic rocks (schists and greywackes), Cambrian chloritized schists, quartzites, greywackes and orthogneisses (dated at 466 ± 10 Ma) and some hyperalkaline syenites, occur within and around CdV (Gonçalves, 1973; Marques et al., 2008). Chromitites, with platinum group elements (PGE), also occur at depth in the study region (Dias et al., 2006). In other ultramafic rock systems, chromitites have been found to contain considerable amounts of abiotic methane and other hydrocarbons (Etiope et al., 2018). These rocks may play an important role in the methane production because of their high content of powerful metal catalysts, such as chromium and ruthenium (Etiope and Ionescu, 2015; Etiope et al., 2018). In the Alter-do Chão massif, PGE-rich chromitites result from two primary deposition events related to progressive fractionation at the dunite to post-dunite stage, represented by stibiopaladinite and froodite, and at lherzolitic stage, coupled by sulphide segregation, causing auricuprite and gold crystallization (Dias et al., 2006). Subsequent platinum-group metals PGM (sperrylite and arsenopaladinite) result from serpentinization repositioning.

Fig. 1 shows the location of the various springs and boreholes in the CdV spa park. They include two boreholes, AC3 and AC5, pumping hyperalkaline mineral water from a depth of 119 m and 126 m, respectively; one hyperalkaline water spring (Ermida); three non-alkaline normal springs (Dos Amores, Borbologão and Sto. António); and a shallow normal water borehole (named Maria Rita).

The AC3 and AC5 boreholes are around 100 m apart from each other, crossing similar geological formations (fissured/fractured serpentinized peridotites). The hydraulic head measured during the construction of the boreholes showed that the potentiometric surface in the area was 1.0 m and 0.1 m above the topographic surface for AC3 and AC5 boreholes, respectively (Cavaco, 1983, 1997). Transmissivity at the CdV discharge area is 4.8 m^2/d at the AC3 borehole and 4.0 m^2/d, at the AC5 borehole (Rocha, 2006). The hydraulic conductivity is 7×10^{-2} m/d (AC3) and 4×10^{-2} m/d (AC5). The AC3 borehole can operate at a maximum flow rate of 1.5 L/s (≈130 m^3/day). The usual operating period is 8 months/year with a mean flow rate (variable depending on the number of spa users) of 50 m^3/day. The AC5 borehole can operate at a maximum flow rate of 0.5 L/s (≈43 m^3/day) for the same operating period, but with a different regularity (from 1 h/day to 12 h/day). The average flow rate is approximately 30 m^3/day. These values seem to be strongly controlled by the fracture network of the ultramafic massif, which is rather highly fractured in the zone of AC3 borehole.

The Ermida spring is well known since the presence of the Romans in the Iberian Peninsula, who exploited the mineral water for therapeutic purposes (Carneiro, 2014). This mineral spring emerges from Cambrian limestones, close to the tectonic contact with ultramafic rocks.

Maria Rita borehole (≈100 m depth) was drilled in the serpentinites, located about 500 m to the N along the alignment of the boreholes AC3 and AC5. It is currently used only for domestic purposes and irrigation. Sto. António spring is located about 20 m from AC3 borehole. Dos Amores and Borbologão springs are about 40–50 m from the boreholes AC3 and AC5, respectively.

2.2. Methodology

We used data: i) gathered in 2002 and published in Marques et al. (2008), ii) aquired in 2012 and published by Etiope et al. (2013b), and iii) unpublished data obtained in 2012, 2013 and 2014. Published data from Marques et al. (2008) include physico-chemical (T ºC, pH, electrical conductivity – μS/cm, major and minor ions and silica) and isotopic analysis (δ^2H, $\delta^{13}C$, $\delta^{18}O$, ^3H and ^{14}C) from AC3 and AC5 boreholes, Ermida spring and other local boreholes and spring waters belonging to different geological formations, such as limestones, gabbros and serpentinites. Published data from Etiope et al. (2013b) include molecular and stable (C and H) isotope composition of methane dissolved in the AC3 and AC5 waters.

Unpublished data have been acquired from 2012 to 2014 from AC3-

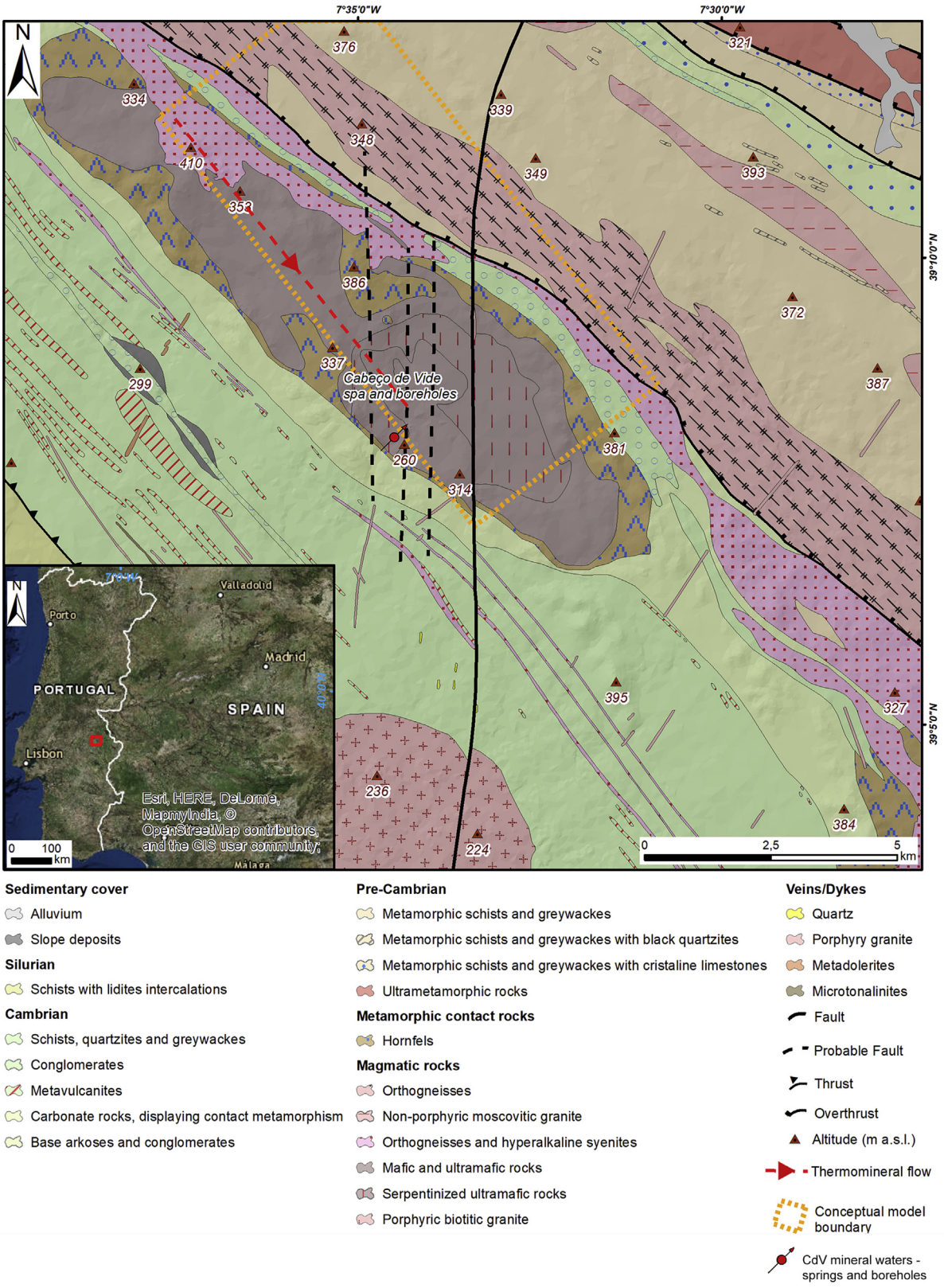

Fig. 1. Location and geologic map of CdV region. Altitude (m a.s.l.) is given through the geodetic marks (△). Adapted from Marques et al. (2008, 2018) and Fernandes J (*pers. comm.*).

AC5 boreholes, Ermida spring, Maria Rita borehole (Fig. 2), Borbologão and Sto. António springs, and also from CdV Stream (Ribeira). They include physico-chemical parameters (T ºC, pH, electrical conductivity - µS/cm, major, minor and trace elements and silica) and isotopic analysis of water (δ^2H, $\delta^{13}C$, $\delta^{18}O$, ^3H and ^{14}C) and molecular and isotopic composition of gas (δ^2H, $\delta^{13}C$). A soil-gas survey was performed in 2014 to verify the occurrence of diffuse degassing of methane from the ground. The new data are presented in Tables S1 (Supporting

Fig. 2. Stream, springs and boreholes sampled in this case study. Surface waters and shallow groundwaters: **(A)** - CdV stream (flowing through serpentinized ultramafic rocks); (B) - Borbologão spring; (C) - Maria Rita borehole. CdV mineral waters: (D) - AC3 borehole; (E) - AC5 borehole; (F) - Ermida spring.

Material), 1 and 2 and Fig. 7.

2.2.1. Water sampling and analysis

Water physico-chemical parameters, including temperature (ºC), pH, oxidation-reduction potential (Eh/mV) and electrical conductivity (EC/µS/cm), were measured *in situ* using digital meters (models WTW-PH330i/set2A20-1011 and WTW- Cond.330i/set2c20-0011, respectively). A few hours after collection, after alkalinity determinations, water samples were filtered with 0.45 µm filters (Millipore). All water samples were stored at 4 °C for later chemical analyses.

The techniques used for water analysis were as follows: inductively coupled plasma mass spectrometry for cations, in HNO_3 acidified samples (pH < 2), performed at Actlabs Laboratory, Canada (Code E6); and ion chromatography for fluoride, chloride, nitrate and sulfate in non-acidified samples, carried out at the Laboratory of Mineralogy and Petrology of the Instituto Superior Técnico (IST), Lisbon (LAMPIST). The alkalinity of the non-acidified samples was determined at LAMPIST, by titration with 0.02 N HCl, using an automatic Metrohm titrator: titration end point pH 8.3 to determine OH^- and/or CO_3^{2-}, followed to titration end point pH 4.5 to determine HCO_3^-, according to Standard Method 2 320B, proposed by APHA (see Arnold et al., 1992).

Environmental isotopes (δ^2H, $\delta^{18}O$ and ^3H) were measured at C^2TN, Campus Tecnológico e Nuclear/Instituto Superior Técnico, Portugal. $\delta^{18}O$ and δ^2H determinations were carried out by laser spectroscopic analysis (LGR 24d) following analytical methods described in IAEA (2009). The isotopic results are reported in the usual δ notation in $^{o}/_{oo}$ *vs.* VSMOW. The accuracy of the measurements is $1^{\circ}/_{oo}$ for δ^2H and

Table 1
Comparison of head space and porous membrane measurements of methane abundances and isotopic compositions in borehole waters at CdV.

Source and Time	Sampling Method	CH_4 (ppm, peak)	$\delta^{13}C$ (per mil)
AC3, 1030	Head space	4137	−21
AC3, 1208	Membrane (3:1)	2400	−22
AC5, 1230	Head space	2230	−24
AC5, 1230	Membrane (3:1)	1200	−25
Maria Rita, 1645	Head Space (West)	12	–
Maria Rita, 1645	Membrane	17	−9

Notes: Membrane measurements from methane rich waters required dilution with 3 parts distilled water. Raw measured values are shown. The improvement in sensitivity was 7x for these measurements, but appeared to be smaller for more dilute waters. Values of $\delta^{13}C$ were not affected by extraction of gases through the membrane.

$0.1^{\circ}/_{oo}$ for $\delta^{18}O$. Tritium (^3H) content in the water samples was determined using an electrolytic enrichment method followed by liquid scintillation counting measurements (PACKARD TRI-CARB 2000 CA/LL CA/LL) with a detection limit of 0.5 TU. The associated error to the measurements (≈0.6 TU) varies with the tritium concentration in the water samples. This analytical method is described in IAEA (1976). Water for radiocarbon dating was sampled in polyethylene bottles (1L/sampling site) and analysed at CAIS - Center for Applied Isotope Studies, University of Georgia (USA) by Accelerator Mass Spectrometry (AMS). For radiocarbon analysis, the dissolved inorganic carbon was extracted in vacuum by acidifying of the water sample. The extracted carbon dioxide was cryogenically purified from the other reaction products and catalytically converted to graphite using the method of Vogel et al. (1984). Graphite $^{14}C/^{13}C$ ratios were measured using the CAIS 0.5 MeV accelerator mass spectrometer. The sample ratios were compared to the ratio measured from the Oxalic Acid I (NBS SRM 4990). The sample $^{13}C/^{12}C$ ratios were measured separately using a stable isotope ratio mass spectrometer and expressed as $\delta^{13}C$ with respect to VPDB, with an error of less than 0.1‰. The quoted dates have been given in radiocarbon years before 1950 (years BP), using the ^{14}C half-life of 5730 years (Aggarwal et al., 2014). The error is quoted as one standard deviation and reflects both statistical and experimental errors. The date has been corrected for isotope fractionation.

2.2.2. Gas analyses

Stable C and H isotope composition of methane ($\delta^{13}C$ *vs.* VPDB; and $\delta^{2}H$ *vs.* VSMOW) dissolved in water from boreholes AC3, AC5 and Ermida spring (May-July 2013) was analysed by isotope ratio mass spectrometry (IRMS; Finnigan Delta Plus XL mass spectrometer, precision ± 0.1‰ for ^{13}C and ± 2‰ for ^{2}H). The stable C isotope ratio of CH_4, and its concentration, dissolved in AC3, AC5 and Maria Rita borehole waters collected in October 2013, was analysed by Cavity Ring Down Spectroscopy (CRDS; Picarro G2112-I CH_4 isotope analyser; precision < 0.7‰ at 1.8 ppmv CH_4, 5 min). CH_4, CO_2, H_2 and C_2-C_5 alkanes concentrations in water were measured, after head-space extraction method (Etiope, 1997), by using respectively (a) a tunable diode laser absorption spectrometer (TDLAS) CH_4 detector (Gazomat, France, assembled in a West Systems sensor package, Italy; precision 0.1 ppmv, lower detection limit 0.1 ppmv); (b) a double beam infrared CO_2 sensor (Licor; accuracy 2%, repeatability ± 5 ppmv and full scale range of 2000 ppmv); (c) a semiconductor H_2 detector (Hydrotech Huberg, Italy; detection limit of 5 ppmv), and (d) a Fourier transform infrared spectrometer (FTIR Gasmet DX-4030, Gasmet, Finland; accuracy around 10%) with typical detection limits of 3 ppmv.

Laboratory TDLAS sensor measurements were corroborated by on-site measurements in October 2013 with a separate Cavity Ring-Down Spectrometer (CRDS, a Picarro G2132-I CH_4 isotope analyser), and at the Jet Propulsion Laboratory using the Carbon Isotope Laser Spectrometer (CILS; Etiope et al., 2013b). In 2014, CILS was deployed *in situ*. To enhance the sensitivity of measurements in both the 2013 and 2014 field campaigns, a silicone hollow fiber membrane module (PermSelect PDMSXA-2500 cm^2) was employed in conjunction with a VWR variable flow peristaltic pump. Except for the most dilute measurements, to avoid saturation of the absorption signal when employing the silicone membrane, it was necessary to dilute with 750 mL distilled water to 250 mL of sampled fluid to produce a gas measurement below the saturation level of the instrumentation. This amounted to roughly a 7x increase in the sensitivity relative to the measurements of headspace gases. This improvement did not appear to scale linearly to low concentrations. The value of $\delta^{13}C$ was unchanged in all membrane measurements relative to the headspace measurements (see Table 1). The use of membranes for gas sampling from fluids may aid in the field detection of methane and quantification of its $\delta^{13}C$, but requires further analysis.

2.2.3. Soil-gas survey

Methane concentrations in soil-air were investigated throughout the CdV spa park, where boreholes and springs are located (see Fig. 7), with the aim of detecting diffuse seepage of the abiotic gas observed in the mineral waters. Soil-gas was sampled using a metallic probe at about 40–50 cm depth in 50 points, homogeneously spaced throughout an area of about 10,000 m^2. The concentration of methane was measured using a multiple sensor system based on semiconductor (range 0–2000 ppmv; lower detection limit: 1 ppmv; resolution: 1 ppmv), catalytic (range: 2000 ppmv to 3 vol%), and thermal conductivity (3–100 vol%) detectors (West Systems, Italy). The stable C isotope composition of soil CH_4 ($\delta^{13}C$-CH_4) was analysed in 2 points (with the highest CH_4 concentrations) by Cavity Ring-Down Spectroscopy (CRDS; Picarro G2112-

Table 2
Molecular and isotopic composition of gas dissolved in the CdV waters.

Sample	Date	pH	CH_4	CH_4	C_2H_6	C_2H_6	CO_2	$\delta^{13}C_{CH4}$		$\delta^{2}H_{CH4}$
			mg/L	*ppmv HS*	*mg/L*	*ppmv HS*	*ppmv HS*	*CRDS*	*IRMS*	*IRMS*
AC3	October 2012	11.23	0.9	3600	0.03	65	600	−18.6	−20.7	−283
"	May 2013	11.58	0.09	250	0.002	7	400	−16.5	−17.1	−285
"	October 2013	11.80	0.7	2500 *(2400)*			350 *(136)*	−23.1		
AC5	October 2012	10.95	0.2–1.2	743–2600	0.002	5	750	−19.8	−23.0	−282
"	May 2013	11.36	0.1	439	0.005	12	440	−21	−22.3	−281
"	October 2013	11.41	0.6	2200 *(1200)*			410 *(0)*	−24.4		
Ermida	July 2013	9.34	0.35	648				−14		−218
Borbologão	May 2013	7.94		< 1.5			3100			
Maria Rita	May 2013	8.44		< 1.5			2900			
Maria Rita	October 2013	10.40	0.003	12 *(17; not dil.)*			490	−9		

Notes – ppmv HS: ppmv in the extracted headspace; *(italic parenthesis are the measurements by CRDS through a silicone membrane, diluted with 1:3 distilled water except where noted).* $\delta^{13}C$ in ‰ *vs.* VPDB; $\delta^{2}H$ in ‰ *vs.* VSMOW; CRDS: Cavity Ring-Down Spectroscopy; IRMS; isotope ratio mass spectrometry. Ethane analyses were by gas chromatography and TDLAS in 2012 (Etiope et al., 2013b), and by FTIR in 2013 (see Methods).

I CH_4 isotope analyser; precision < 0.7‰ at 1.8 ppmv CH_4, 5 min).

2.2.4. Microbial analyses

The microbial communities associated with the mineral waters from CdV were analysed by DNA-based analysis to understand the interactions between microbes and geochemical settings occurring at this site. Microbial samples were collected from the borehole AC3 by filtration using peristaltic pumps to collect water with Tygon E-LFL tubing (Masterflex) and 47 mm in-line filter holders (0.22 µm pore-size filters). After filtration (approximately 4–5 h), the filters were aseptically placed into sterile tubes and stored on ice during transportation. Filter samples for morphological characterization of microbial cells were dried at 30 °C, sputter coated with a Cr film and observed under Field Emission Scanning Electron Microscopy (FESEM) with Energy Dispersive X-ray Spectroscopy (EDS). FESEM examinations were performed using a Jeol JSM-7001F microscope (Jeol, Tokyo, Japan) equipped with an Oxford EDS detector (Oxford Microbeam, Oxford, UK), which was operated using the secondary electron (SE) detection mode with an acceleration voltage of 15 kV.

The membrane filters for DNA-based analysis were used for DNA extraction using the FastDNA® SPIN for Soil Kit (MP Biomedicals, France) in conjunction with the FastPrep® instrument, following the manufacturer's protocol. The prokaryotic 16S rRNA gene was amplified by Polymerase Chain Reaction (PCR) using the primer pair 616F (5′-AGAGTTTGATYMTGGCTCAG-3'; Snaidr et al., 1997) and 1510R (5′-GGTTACCTTGTTACGACTT-3'; Lane, 1991). The PCR reactions were performed in 50 µL volumes, containing 5 µL of 10x PCR buffer, 2 µL of 50 mM $MgCl_2$, 5 µL of 2 mM dNTP mix (Invitrogen, Carlsbad, CA, USA), 0.5 µL of 50 µM of each primer (Macrogen, Seoul, Korea), 10–20 ng of the extracted DNA as template, 1.25 units of Taq DNA polymerase (Bioline, GC Biotech, The Netherlands), and sterile ultrapure water. PCR amplifications were performed in a BioRad iCycler thermal cycler (BioRad, Hercules, CA, USA) using the following cycling parameters: 2 min of initial denaturing step at 95 °C, followed by 35 cycles of denaturing (95 °C for 15 s), annealing (55 °C for 15 s) and extension (72 °C for 2 min), with an additional extension step at 72 °C for 10 min. All PCR products were inspected by agarose gel 1% (w/v) electrophoresis, stained with SYBR Green I (Roche Diagnostics, Mannheim, Germany) and visualized under UV light. Positive PCR products were purified using the JetQuick PCR Purification Spin Kit (Genomed, Löhne, Germany) and cloned with the TOPO TA Cloning Kit (Invitrogen, Carlsbad, CA). Clones were sequenced by Macrogen Europe (Amsterdam, The Netherlands) to further determine their phylogenetic affiliations. DNA sequences were edited with the BIOEDIT v7.0.4 software (Technelysium, Tewantin, Australia) and aligned using MUSCLE (Edgar, 2004). Aligned sequences were clustered into operational taxonomic units (OTUs) using the program DOTUR (Schloss and Handelsman, 2005), based on a 97% sequence identity cut-off. A homology search of the sequences was performed using the BLASTn algorithm (Altschul et al., 1990) of the NCBI database and SILVA database. A Neighbor-Joining phylogenetic tree was constructed using MEGA7 (Kumar et al., 2016) by heuristic search. Closest relatives were collected from SILVA as reference sequences for creating the phylogenetic tree. Bootstrap values were generated from 1000 replicates. Sequences were submitted to the European Nucleotide Archive (ENA, EMBL-EBI) under the accession numbers from LT969602 to LT969610.

3. Results and discussion

3.1. Physico-chemical features of spring and borehole waters

Associated with the intrusion of the Alter-do-Chão mafic/ultramafic pluton, and from the border to the core (see Fig. 1) groundwaters show the following features:

i) Groundwaters issuing within the Cambrian limestones are Ca-HCO_3-type waters with neutral to slightly basic pH, and medium to high mineralization, with EC values between 663 and 841 µS/cm (see Marques et al., 2008);
ii) Groundwaters associated with local gabbroic rocks have a Ca/Mg-HCO_3 *facies* (Marques et al., 2008), present neutral pH values and have medium mineralization. Some springs are located at the geologic contact with the metamorphosed limestones;
iii) Local Mg-HCO_3-type waters constitute most of the surface (CdV stream) and shallow groundwaters discharging from the serpentinites (see Table S1 (Supporting Material));
iv) Within the contact between the metamorphosed limestones and the mafic/ultramafic pluton (Fig. 1), CdV mineral waters discharge with temperatures between 17 and 20 °C. These mineral waters present very alkaline pH values (pH > 10.5) and electrical conductivity values between 400 and 650 µS/cm. The CdV hyperalkaline mineral waters are characterized by high Ca^{2+}, $Na^+ + K^+$, and chloride concentrations, presenting a Na-Cl/Ca-OH *facies*. Other main chemical characteristics are: i) hydroxide and carbonate were only detected in the CdV hyperalkaline mineral waters, and ii) the presence of extremely low Mg^{2+} and silica concentrations.

In the Ca-HCO_3-type waters, the Mg/Ca ratio is close to 0.5, reflecting interaction with calcites, the main mineral of the carbonate rocks (see Marques et al., 2008). The Mg concentrations can be attributed to the presence of dolomite (Fig. 3a and b). In the contact between the Cambrian limestones and the ultramafic body, the metamorphosed limestones (contact metamorphic aureoles) have no water, as revealed by a dry borehole (≈189 m depth) drilled in this area. It seems that the contact metamorphic aureoles act locally as a hydrogeological barrier due to the lower permeability of the crystalized limestones (marbles). This hydrogeological configuration is important for promoting the ascent of mineral waters through the contacts between the ultramafic rocks and marble, and contributing to the low vulnerability of the deep mineral aquifer to pollution by shallow groundwaters from the carbonate aquifer system.

Serpentine dissolution might explain the high Mg^{2+} and SiO_2 concentrations found in the local Mg-HCO_3-type waters (e.g., Barnes et al., 1967; Barnes and O'Neil, 1969), which are strongly undersaturated with respect to chrysotile (Marques et al., 2008),

$$Mg_3Si_2O_5(OH)_4 + 6H^+ = 3Mg^{2+} + 2H_4SiO_4^0 + H_2O$$

(*chrysotile*)

suggesting that water chemistry is strongly host rock dependent (see Fig. 3a and b). As described by Barnes et al. (1967, 1972), in regions where ultramafic rocks dominate, groundwater chemistry is essentially a function of the mineral composition of the aquifer through which it flows. Deep circulation through the ultramafic rocks leads to serpentinization (olivine and pyroxene hydration). As groundwater moves along its path from recharge to discharge areas, a variety of hydrogeochemical processes can change its chemical composition (e.g., Hem, 1970). Because the chemical composition of groundwater reflects the water-rock interaction and chemical processes, groundwater chemistry can be used to identify the main water-rock interactions occurring in the study region.

CdV hyperalkaline mineral waters with moderate mineralization, as indicated by the electrical conductivity values (see Fig. 3c and Table S1 (Supporting Material)), are a distinctive indication of active serpentinization. Their chemistry is controlled by the liberation of OH^- and Ca^{2+} during the hydration of olivine and pyroxenes in ultramafic rocks, resulting in typical Na-Cl/Ca-OH *facies* (see Fig. 3 d, e and Table S1 (Supporting Material)), largely driven by meteoric waters (e.g., Barnes and O'Neil, 1969; Bruni et al., 2002; Chavagnac et al., 2013). The effluent temperatures of CdV mineral waters are typical of continental peridotite-hosted groundwaters, where geothermal gradients are relatively low (e.g., Chavagnac et al., 2013; Etiope, 2017a and references

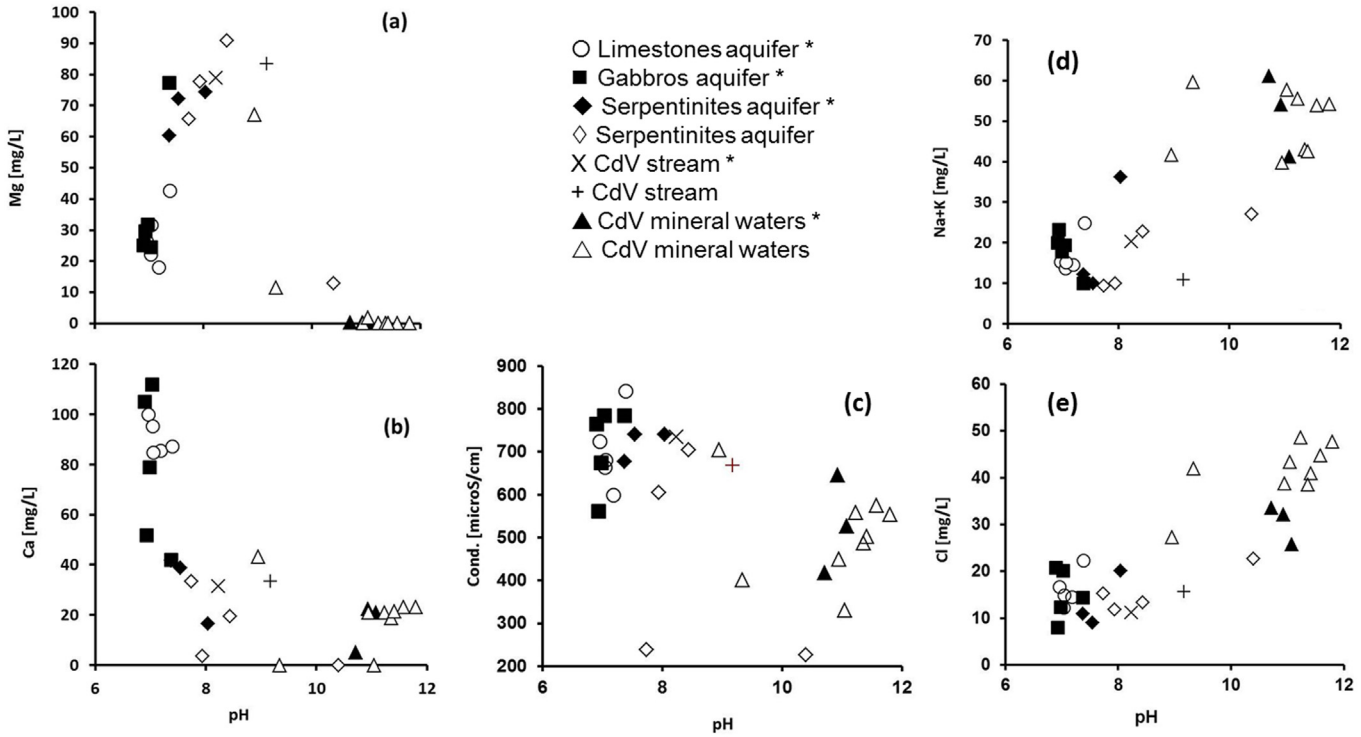

Fig. 3. (a) Mg *vs.* pH, (b) Ca *vs.* pH, (c) Cond. *vs.* pH, (d) Na + K *vs.* pH and (e) Cl *vs.* pH relationships in surface waters, shallow and deep groundwaters from CdV region. (*) Data from Marques et al. (2008).

therein).

As stated by Barnes et al. (1967), the serpentinization of the ultramafic rocks (Fig. 4) might contribute to the development of such type of mineral waters, characterized by very low silica and Mg^{2+} concentrations:

$$\underset{(forsterite)}{2Mg_2SiO_4} + 3H_2O = \underset{(brucite)}{Mg(OH)_2} + \underset{(chrysotile)}{Mg_3Si_2O_5(OH)}$$

The serpentinization is driven by meteoric water infiltration (present-day serpentinization), according to models proposed by Barnes et al. (1967, 1972), Bruni et al. (2002) and Marques et al. (2008). The general process of serpentinization can be described by the overall reaction:

olivine + pyroxene + H_2O → serpentine ± brucite ± magnetite + H_2

Where serpentine means one or more members of a mineral group that includes lizardite, antigorite and chrysotile (e.g., McCollom and Seewald, 2013). The minero-petrographic studies performed on drill cores from CdV, AC3, and AC5 boreholes corroborate this model, with most of the Mg^{2+} and SiO_2 retained in serpentines and vein brucite. Because olivine is stable in the presence of water at high temperatures, serpentinization is limited to temperatures below 330–400 °C, depending on the pressure (McCollom and Bach, 2009).

Fig. 4. Drillcore from the exploration borehole AC2 (CdV Spa). Serpentinized peridotite, showing strong serpentinization along the rock fractures.

CdV mineral waters should be linked to a deeper ultramafic aquifer system, where slow-flowing groundwaters promote serpentinization today through water-rock interaction with fresh dunites/peridotites, along additional water transport pathways such as a fissure/fracture network (e.g., Malvoisin and Brunet, 2014). In fact, geofluids discharging from active, low-temperature serpentinization sites have some of the highest pH values ever documented in natural systems (e.g., Mottl et al., 2003; Etiope and Sherwood Lollar, 2013; Etiope et al., 2017 and references therein). As a consequence, the springs are often surrounded by calcite ($CaCO_3$) precipitation (Fig. 2F) as CO_2 from the atmosphere is absorbed into the alkaline fluids (Bruni et al., 2002; Mottl et al., 2003; Cipolli et al., 2004; Etiope and Sherwood Lollar, 2013). As stated by Sanchez-Murillo et al. (2014), such calcite deposits precipitated at the exit sites of the hyperalkaline spring waters, are typical features that indicate that present-day serpentinization is occurring in the subsurface.

An understanding of the geochemical evolution of mineral waters is also important for its sustainable development as a public resource. In this connection, the present research work has also been conducted with the aim of assessing the chemical components of the different types of groundwaters in CdV region, in order to contribute to the sustainable management of the mineral aquifer system. In the diagrams of Fig. 3 we can observe that the CdV mineral waters (△) from Ermida spring (data from 10/2013 – see Table S1 (Supporting Material)) are detached from the group of CdV mineral waters, evidencing a possible mixing process with the local shallow groundwaters. This mixing process is evidenced by an increase in Mg^{2+}, Ca^{2+} and electrical conductivity and a decrease in pH. In this likely mixing process, the mineral water from Ermida spring approaches the chemical composition of the local shallow Mg-HCO_3-type groundwaters. Usually, thermal

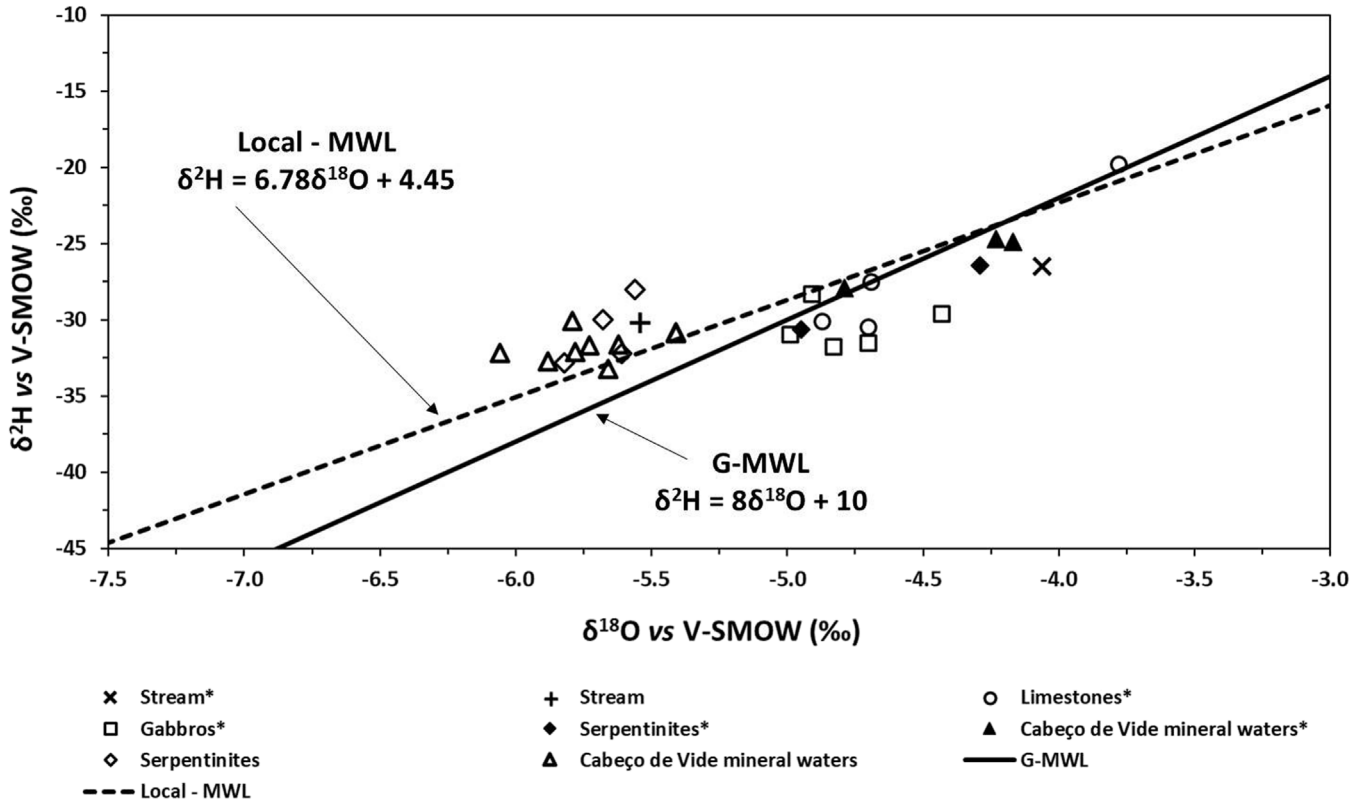

Fig. 5. δ^2H *vs.* $\delta^{18}O$ relationship in water samples from the CdV region. * Data from Marques et al. (2008).

spring waters are much more vulnerable to mixing with shallow groundwaters than thermal borehole waters, due to their slower ascending flow path. On the other hand, thermal borehole waters are extracted from deep boreholes (with casing that is cemented in place) crossing rock discontinuities (fractures and/or faults), and their sustainable development is not so strongly dependent on water protection, waste and leakage prevention, water withdrawal and exploitation within the system limits as in the case of thermal spring waters (e.g., Voronov and Vinograd, 2009; Gultekin et al., 2011). Potential hydrological connectivity between the local shallow Mg-HCO_3-type groundwater system and hyperalkaline spring seepage deviation was detected in 10/2013, related to the overexploitation of the local Mg-HCO_3-type shallow groundwaters from boreholes (e.g., Maria Rita borehole waters), due to an extreme dry season. In fact, as shown in the diagrams of Figs. 3–5, the waters (◊) from Maria Rita borehole (data from 10/2013) are characterized by a pH of 10.4 and an uncommon chemical composition (see Table S1 (Supporting Material)), approaching the CdV mineral water signatures as revealed by the unusual higher Na^+ and Cl^-, and lower Mg^{2+}, HCO_3^- and SiO_2 values. This trend suggests a possible mixing process with the CdV mineral waters.

3.2. Water origin and age

3.2.1. Water stable isotope composition

Isotopic ($^{18}O/^{16}O$ and $^2H/^1H$) ratios were used to estimate the relative importance of locally infiltrated meteoric waters to the recharge of the CdV mineral waters. For most of the samples, the concentrations of the stable isotopes (δ^2H and $\delta^{18}O$) in CdV mineral waters (Fig. 5) follows the Global Meteoric Water Line (GMWL: $\delta^2H = 8\ \delta^{18}O + 10$) defined by Craig (1961), later improved by Rozanski et al. (1993), Bowen and Wilkinson (2002) and more recently by Terzer et al. (2013). The water stable isotopic composition also fits the relationship in the Local Meteoric Water Line (LMWL: $\delta^2H = 6.78\ \delta^{18}O + 4.45$) established with the monthly precipitation database from Portalegre IAEA-WMO station between 1988 and 2004 (Carreira et al., 2005). This station is located about 15 km to NE of CdV research area.

The stable isotope results indicate that i) all groundwater samples, independent of their composition, are meteoric waters, and ii) there is no evidences of water-rock interaction at high temperatures, no ^{18}O enrichment due to water-rock isotopic equilibrium is detected within these samples, consistent with the low issue temperature of the CdV mineral waters.

In each campaign (2002 and 2012–2013) the local shallow Mg-HCO_3-type groundwaters discharging from the serpentinized peridotites, and the CdV mineral waters have similar δ^2H and $\delta^{18}O$ values (see Fig. 5), indicating that the CdV mineral waters could have evolved from deep infiltration, along major faults/fractures, of the shallow Mg-HCO_3-type groundwaters, as previously stated by Marques et al. (2008). A similar trend was observed by Cipolli et al. (2004) and Sanchez-Murillo et al. (2014). An isotopic depletion of the groundwater samples from the 2012–2013 field work campaigns (Fig. 5) (around 1‰ in ^{18}O and 5‰ in ^2H) as compared with the earlier samples from the same locations can be attributed to the different isotopic methods used in each campaign: in 2002 (data presented by Marques et al., 2008) a mass spectrometer SIRA 10 was used for the isotopic determinations of water samples, while for 2012–2013 water samples employed a Laser Water Analyser LGR 24d.

3.2.2. Water dating

The tritium content measured recently (2012–2013 campaigns) in the groundwater samples, either from the CdV mineral aquifer system or from the shallow serpentinite aquifer (Mg-HCO_3-type waters) varies between 0 and 1.4 ± 0.8 TU (Maria Rita borehole - Mg-HCO_3-type waters), with 1.1 ± 0.3 TU in Ermida spring (mineral waters). From these concentrations, it is possible to conclude that the mean residence time in both aquifer systems is more than 60 years. The tritium record in the region (1988–1999 time series) has a mean content of 5.3 TU. We assume a piston flow model (Carreira et al., 2007).

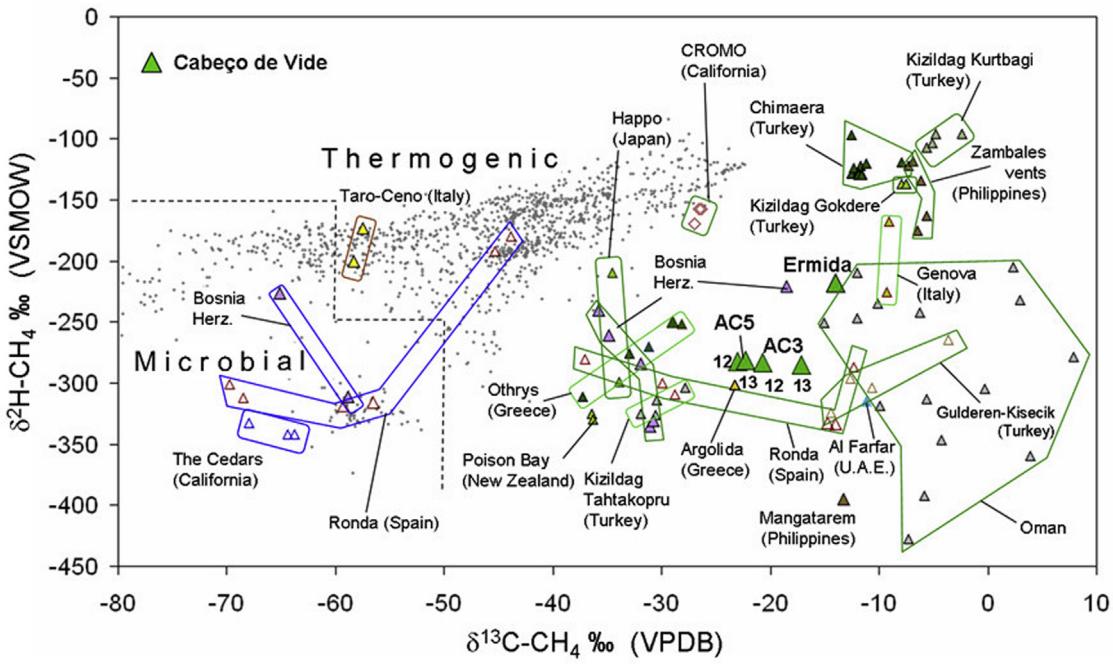

Fig. 6. $\delta^{13}C_{CH4}$ *vs.* $\delta^{2}H_{CH4}$ diagram of CdV mineral waters compared with other continental serpentinization sites documented so far, and biotic (microbial and thermogenic) methane from sedimentary basins (grey dots). Data from Etiope et al. (2017) and Vacquand et al. (2018).

Marques et al. (2008) reported $\delta^{13}C$ and ^{14}C data for CdV mineral waters. The $\delta^{13}C$ values were -22.9‰ and -18.0‰ for boreholes AC3 and AC5, respectively. The ^{14}C values ranged between 69.12 ± 0.28 pmC and 65.24 ± 0.35 pmC (AC5 and AC3 boreholes, respectively). New $\delta^{13}C$ and ^{14}C data from 2013 field work campaign are presented in Table S1 (Supporting Material).

The piston model developed by Marques et al. (2008), a close model to the CO_2, in the calculation of CdV mineral waters ages, indicates apparent groundwater ages of 3.6 ± 2.3 ka BP and 6.0 ± 2.2 ka BP for AC5 and AC3 boreholes, respectively. They assumed that the recharge occurs in two stages: i) a first stage concerning the reactions occurring during water infiltration in the unsaturated zone, an open system for isotopic exchange via the soil zone and the free atmosphere, and ii) a second stage of storage, in which the water is subjected to secondary hydrochemical reactions and resulting aging in a closed geochemical system. In this appraisal the carbon-13 content of the TDIC (Total Dissolved Inorganic Carbon) was used as correction factor, as well as the ^{13}C content of the soil and of the rock matrix (Salem et al., 1980; Gonfiantini and Zuppi, 2003).

In the present study, using the $\delta^{13}C$ and ^{14}C data from 2013 field sampling campaign and the same correction model used by Marques et al. (2008), younger apparent groundwater ages were obtained, namely for borehole AC3 = 1.9 ± 1.2 ka BP and for borehole AC5 = 1.5 ± 1.2 ka BP. The ^{14}C data (98.23 ± 0.42 pmC) for Ermida spring point to a modern age. As seen in the deviation of the chemical signatures of the mineral waters during the 2013 campaign, variation in the carbon-14 and enrichment in the carbon-13 content is observed, compared with the data presented by Marques et al. (2008). An anti-aging "factor" is identified; the apparent carbon-14 ages are much younger, around 2 to 4 ka younger.

As already mentioned, 2013 was a very dry year, which induced increased groundwater use from all aquifer units in the region. The overexploitation of CdV mineral waters tended to lower the piezometric surface and increase the amount of percolation through the separate adjacent aquifers, changing the ^{14}C and ^{13}C content and consequently the ^{14}C apparent ages of the mineral waters. Similar changes were mentioned by Geyh (2000). The author focused on the apparent mobilization and mixing of groundwaters from different depths or from different aquifers due to overexploitation.

According to Geyh and Kunzl (1981), the presence of methane within the groundwater systems increases the groundwater ^{14}C apparent ages if the fossil organic matter has been decomposed to methane. This also changes the ^{13}C content in the TDIC. These authors also note that about 50 µmol/L of CH_4 in the groundwater system (fossil origin) can increase the ^{14}C age by 160 yrs if no gas is lost during the sampling and measurement. In CdV mineral waters, the highest concentration of methane is 1.2 mg/L (see item 4.3), and no fossil organic matter has been reported (e.g., Marques et al., 2008; Etiope et al., 2013b). In this situation, and assuming a fossil origin for the CH_4, this amount of methane (maximum content of 75 µmol/L) can increase the apparent ages of the groundwater (dilution of the percentage of modern carbon in the groundwater system) by about 240 years. However, as mentioned above no fossil organic matter had been reported, and the isotopic data are typical of abiotic CH_4 origin, supporting a predominantly non-microbial source (see section 3.3).

3.3. Gas occurrence and origin

3.3.1. Gas chemistry and methane isotopic composition

The results of the gas analyses are reported in Table 2. The analyses of the gas dissolved in AC3 and AC5 boreholes performed in 2013 confirm (a) the ^{13}C enrichment in CH_4 observed in 2012 (Etiope et al., 2013b), and (b) the very low concentrations of CO_2 (not distinguishable from atmospheric equilibrium values) and H_2 (below detection limit of 5 ppmv in the extracted headspace; not reported in Table 2). CH_4 concentrations were higher in autumn (AC3: 0.7–0.9 mg/L, AC5: 0.6–1.2 mg/L in October 2012 and 2013) and lower in spring (AC3: 0.09 mg/L; AC5: 0.1 mg/L in May 2013).

Methane dissolved in the Ermida spring is more ^{13}C and ^{2}H enriched compared to CH_4 of AC3-AC5 boreholes. This could be an effect of CH_4 oxidation due to the very low (≈0.07 L/s) flow rate of the spring water. The $\delta^{13}C$-$\delta^{2}H$ pair of Ermida (Fig. 6) would be compatible with a microbial oxidation trend starting from $\delta^{13}C$-$\delta^{2}H$ of AC3-AC5 values. Methane in the Borbologão spring was below the detection limit (< 1.5

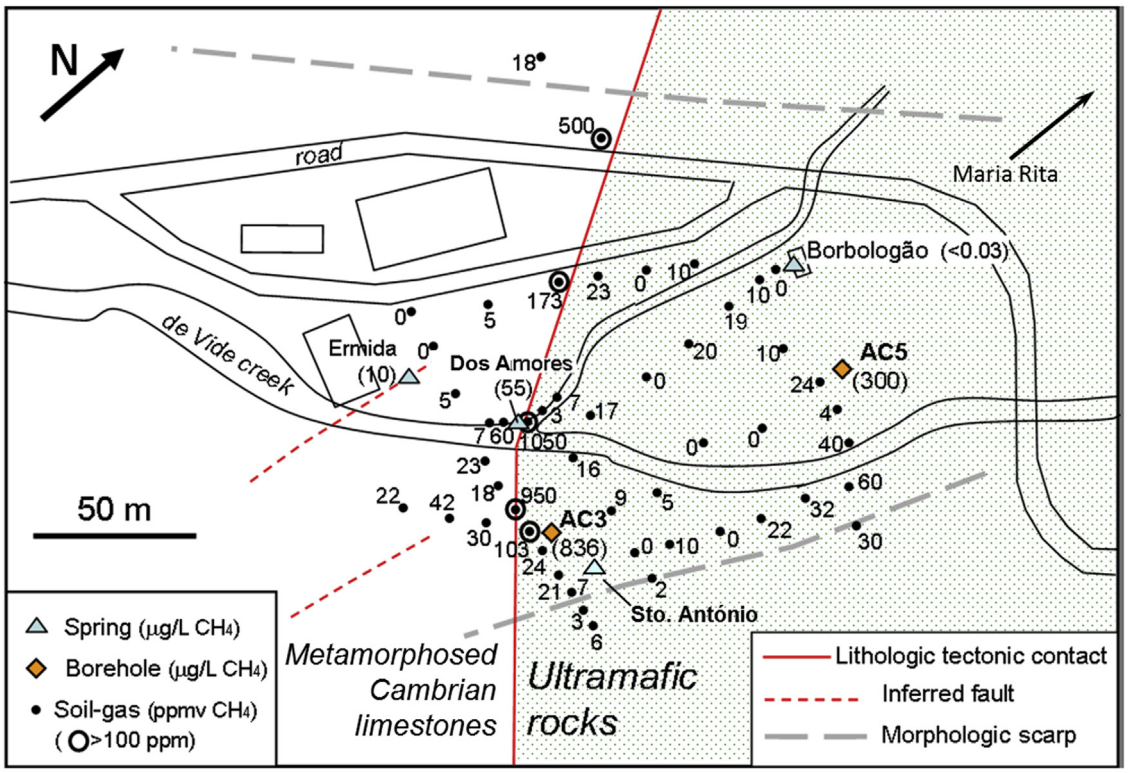

Fig. 7. Methane concentration in soil-air was throughout the CdV Spa Park, where boreholes (AC3[1] and AC5[1]) and springs (Ermida[1], Dos Amores, Sto. António and Borbologão) are located, with the aim of detecting diffuse seepage of the abiotic gas observed in the [1]mineral waters.

ppmv). The shallow (≈100 m deep) Maria Rita borehole water showed an interesting behavior: in May 2013 the CH_4 concentration was below the detection limit, when pH was 8.4, but it increased to 12–17 ppmv in October 2013 when pH was 10.4. The δ^{13}C-CH_4 value was -9‰.

The increase of pH and CH_4 concentration in Maria Rita borehole waters may be explained by episodic upwelling of the deep hyperalkaline mineral waters, and its mixing with the shallower aquifer due to increased pumping and overexploitation of the shallow Mg-HCO_3-type waters, used by the local population for agriculture and cattle breading, at the end of an extreme dry year (2013). This suggests that non-hyperalkaline springs or shallow boreholes may episodically turn into methane-rich water discharges if they are "contaminated" by the deeper hyperalkaline aquifer. Overall, the concentrations of methane (0.35–1.2 mg/L; 22–75 μM) and its isotopic composition ($-24.4‰ < \delta^{13}$C-$CH_4 < -14.0‰$ and $-285‰ < \delta^{2}$H-$CH_4 < -218‰$) in the CdV waters are within the range of values typically observed in peridotite-hosted hyperalkaline waters (Fig. 6). The isotopic data are typical of abiotic CH_4 origin. The low C_1/C_2 ratio (40 and 35 in AC3 and AC5 boreholes, respectively) would support a predominantly non-microbial source. CRDS measurements agreed with CH_4 and δ^{13}C values at AC3 and AC4.

3.3.2. Methane-water isotope disequilibrium

Based on δ^{2}H-CH_4 and δ^{2}H-H_2O, the CH_4-H_2O (aq) fractionation factor α, following the equations and notation of Horibe and Craig (1995), is about 0.739 corresponding to an equilibrium temperature of -8 °C. This is obviously unrealistic and it means that CH_4 did not interact with water for a time sufficiently long to reach isotope equilibrium. Similar methane-water disequilibria are generally observed in serpentinized peridotite systems (Etiope et al., 2017). This would support the hypothesis that CH_4 is allochthonous, not generated in the hyperalkaline water system, as required by non-aqueous rules of the Sabatier reaction (Etiope, 2017b).

3.3.3. Diffuse emission of methane from the ground

Soil-gas analyses show methane concentrations in soil, at a depth of about 0.5 m, ranging from 0 to 1050 ppmv (Fig. 7). Concentrations above the atmospheric level (2 ppmv) were recorded in about 70% of the measured points. The highest values, exceeding 100 ppmv, correspond with the NW-SE tectonic contact between sedimentary rocks (the Cambrian limestones) and ultramafic rocks (a cumulate-type structure of Ordovician age), which crosses the site of the CdV spa near the AC3 borehole (Fig. 7). Concentrations of 500 ppmv were detected about 100 m from the boreholes and springs. The data show that methane is seeping diffusely from the ground with a channelled seepage along the tectonic contact. Similar gas-phase emissions along faults were observed in several serpentinized ultramafic rock systems, such as the Tekirova ophiolite (Turkey: Etiope et al., 2011), Othrys ophiolite (Greece; Etiope et al., 2013a) and Ronda peridotite massif (Spain; Etiope et al., 2016). This means that methane is not only transported to the surface by the hyperalkaline water.

3.3.4. Modeling methane origin

The main gas-geochemical model that can explain the origin of methane in these systems is based on the assumption that the gas is produced by Fischer-Tropsch Type reactions, the Sabatier reaction in particular, where H_2 produced by serpentinization reacts with CO_2 that may derive from multiple sources (dissolution of carbonate rocks, biogenic sources or mantle degassing, depending on the geological setting of the area). In the CdV area, limestone formations, surrounding the Alter-do-Chão intrusive massif, are in contact metamorphism with the serpentinized ultramafic rocks, as described in Section 2. The abiotic reaction must occur in the presence of metal catalysts, generally Fe, Ni and Cr, if temperatures are higher than 150–200 °C, or ruthenium (Ru) if temperatures are lower than 100–150 °C (Etiope and Ionescu, 2015; Etiope et al., 2017). The maximum depth of the serpentinized peridotites in the Alter do Chão ultramafic massif, within which methane was likely produced, is about 1 km (Pinto et al., 2004),

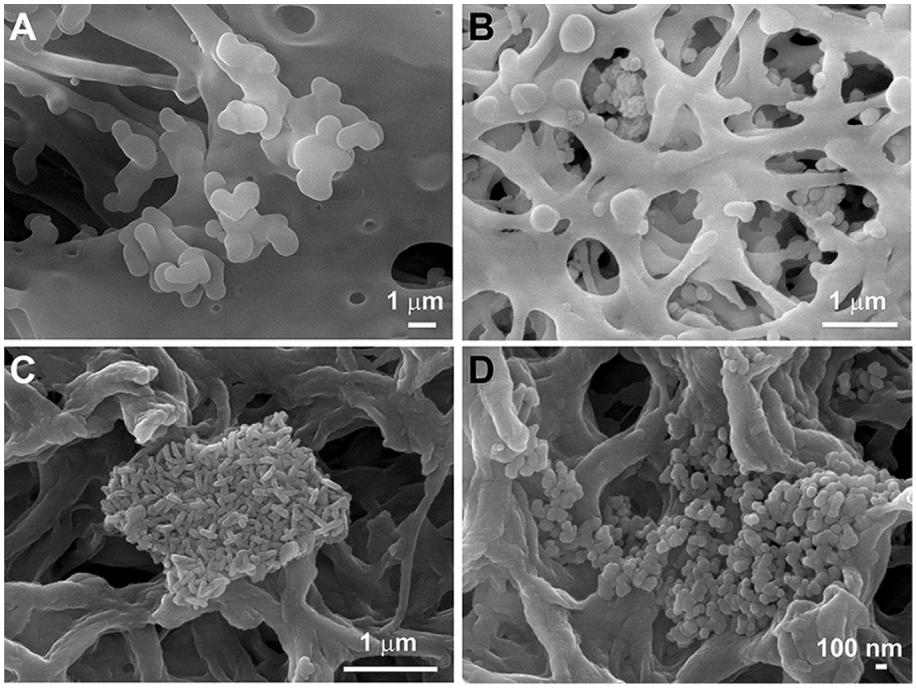

Fig. 8. FESEM images of CdV mineral waters collection filters showing: A) rod-shaped cells; B) nanosize bacteria-like particles; C) clusters of rod-shaped and D) globular cells of putative nanobacteria.

corresponding to a hydrostatic pressure of 96 bar, well below the critical pressure of water. Assuming the local present-day geothermal gradient of about 30 °C/km (IGM, 1998), the depth of 1 km corresponds to temperatures below 50 °C. This is compatible with the low temperatures of the CdV spring waters (~20 °C), and the typical temperatures associated with other continental gas-bearing serpentinization systems (Etiope et al., 2011, 2017). Serpentinization and related gas production in the Alter do Chão ultramafic massif may have occurred at any time during the Myr thermal evolution (cooling) of the igneous intrusion, so the actual gas formation temperature could be higher. The earliest serpentinization may have begun soon after the emplacement of the Alter do Chão ultramafic massif, given that inherent rock fracturing would have favoured the infiltration of meteoric waters at great depths. Clumped-isotope CH_4 analyses (Young et al., 2017) have, however, revealed that methane at CdV is in isotopologue disequilibrium, with very low $\Delta^{12}CH_2D_2$ values (-7.57) resembling those of methane produced by low-temperature non-aqueous abiotic synthesis in the laboratory (see Fig. 14 in Young et al., 2017). Like other abiotic gases, such as those in Canadian Precambrian shields where CH_4 was produced at around 30–40 °C (Young et al., 2017), the CdV methane likely migrated into cool water, where the low $\Delta^{12}CH_2D_2$ signature was preserved. The low T isotopologue signature is not compatible with the magmatic (high temperature) fluid inclusion source model suggested for submarine hot springs by Wang et al. (2018). Assuming a catalysed abiotic synthesis (Sabatier reaction), the low temperature CH_4 production needs appropriate catalysts, such as ruthenium sulfides or oxides, which are particularly abundant as Platinum Group Minerals (PGM) in chromitites. PGM-rich chromitites have been, actually, found to be source of methane in ophiolites in Greece (Etiope et al., 2018). These rocks also occur in the Alter do Chão massif (Dias et al., 2006) and could therefore be a source of the methane observed in the hyperalkaline water.

3.3.5. Hydrogen paucity

The generation of H_2 during serpentinization is related to Mg-rich forsterite olivine and pyroxene through Fe^{2+} oxidation and magnetite (Fe_3O_4) formation (e.g., McCollom and Bach, 2009), a process that can be summarized by the following reaction:

$$2(Fe^{II}O)_{rock} + H_2O \rightarrow (Fe^{III}_2O_3)_{rock} + H_2$$

H_2 would represent the H feedstock for CH_4 production. Its abundance varies in hyperalkaline waters and gas seeps in continental serpentinization systems: high concentrations occur in Oman, Turkey, New Zealand, the Philippines, the United States, Bosnia, and Herzegovina; and lower concentrations, even below detection limits, were documented in Italy, Spain, and Greece. CdV is an additional case of low H_2. The paucity of H_2 can be due to its complete consumption by CO_2 reduction (Sabatier reaction) in a limited or decreased H_2 production system. H_2 can, however, be consumed by specialised microbes, which have been detected in the CdV water as reported below.

3.4. Microbial processes

The H_2 and CH_4 produced within serpentinites can provide metabolic energy for microbial communities in serpentinization sites (e.g., McCollom, 2007; Morrill et al., 2013; Suzuki et al., 2013, 2014). Meanwhile, water discharged from the system is often highly-alkaline, which restrains the microbial metabolic activities. Terrestrial serpentine-hosted alkaline springs support microbial communities, and the microbiology of these systems has been recently described (Brazelton et al., 2012, 2013, Tiago and Veríssimo, 2013). Ultra-basic (pH ≈ 11–12) reducing (-656 to -585 mV) groundwater springs discharging from serpentinized peridotite of The Cedars, California, USA, were investigated for their geochemistry and geobiology (Morrill et al., 2013; Suzuki et al., 2013, 2014, 2017). The results obtained indicated that all of the springs were very low (≤1 μM) in several essential elements and electron acceptors (e.g., nitrate/ammonium, sulfate, and phosphate) required for (microbial) growth, which is not uncommon at sites of continental serpentinization. Those authors also concluded that the ultra-basic and highly reducing springs are habitable for microorganisms.

FESEM images of microbiological samples collected from CdV mineral waters showed that coccoid and rod-shaped cells (≈1 μm) were infrequent (Fig. 8 A), while smaller microbial cell-like structures

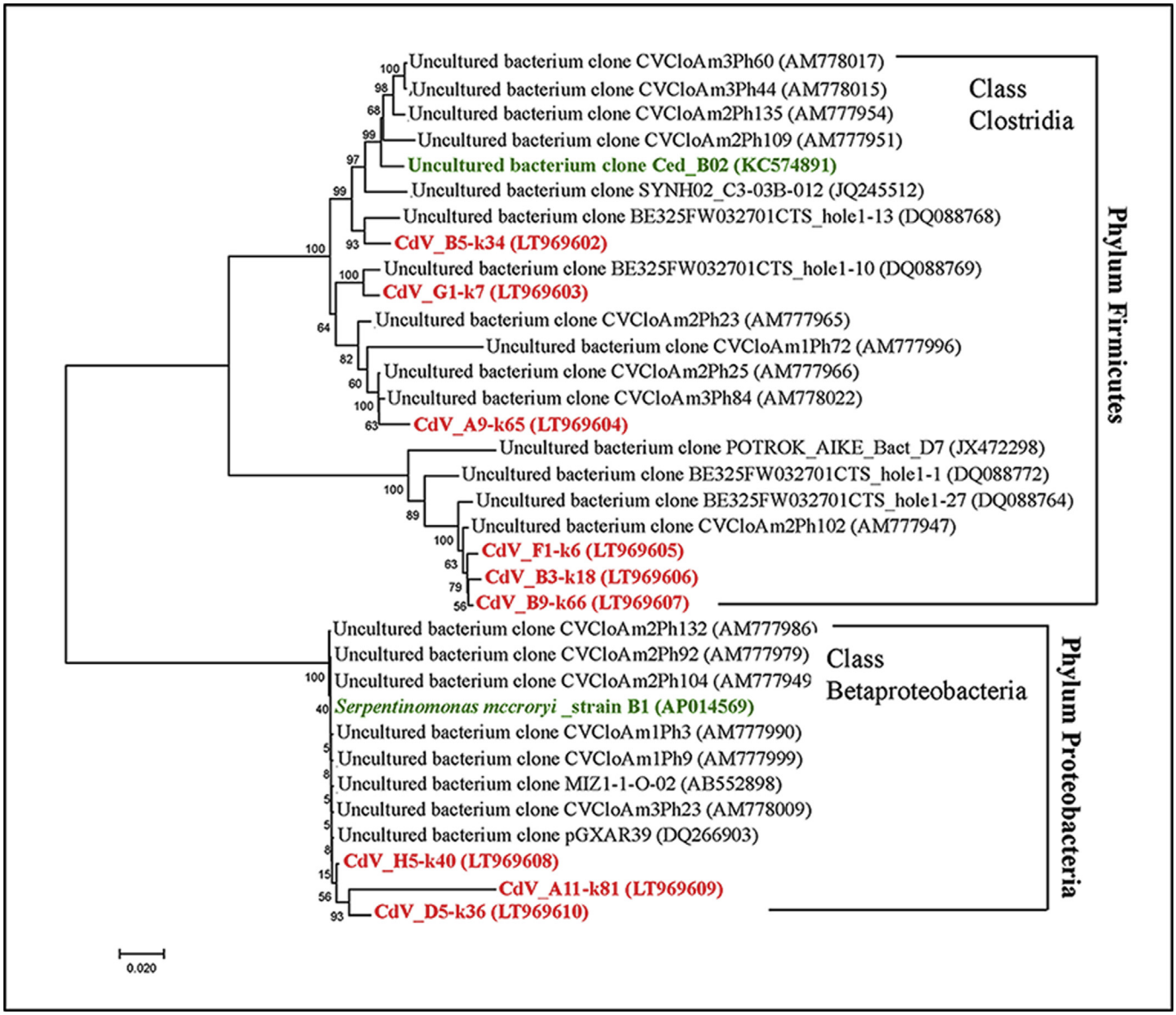

Fig. 9. Neighbor-Joining phylogenetic tree derived from 16S rRNA gene sequences showing the relationships between the dominant clones retrieved from CdV (in red color) and closest relative sequences extracted from SILVA database belonging to Clostridia and Betaproteobacteria classes. Names in green color correspond to clones recovered from the terrestrial serpentinization site of The Cedars by Suzuki et al. (2014). (For interpretation of the references to color in this figure legend, the reader is referred to the Web version of this article.)

(≈0.1–0.2 μm) were abundant (Fig. 8 B, C, D). These putative nanosize bacteria appear with globular (Fig. 8 B) and rod shapes (Fig. 8 C), forming clusters (Fig. 8C, D). Energy dispersive X-ray microanalysis of nanoforms showed C and Ca peaks (data not shown).

The identification of microbial communities by 16S rRNA gene analysis confirmed that the mineral waters from CdV (AC3 borehole) are dominated by members of the class *Clostridia*, phylum *Firmicutes* (Fig. 9) as previously reported by Tiago and Veríssimo (2013).

16S rRNA genes retrieved from the CdV hyperalkaline aquifer (borehole AC3) were closely related to the isolate named '*Serpentinomonas mccroryi* strain B1' (Fig. 9), which was originally isolated from The Cedars serpentinization site and known as a hydrogen oxidizing alkaliphlic bacterium (Miller et al., 2016; Suzuki et al., 2014). In this context, microbial H_2 consumption may occur in the CdV mineral waters. We further successfully cultivated several environmentally-relevant *Serpentinomonas* strains whose 16S rRNA genes are mostly identical with the OTU1 (identity = 98–100%) previously reported by Tiago and Veríssimo (2013). According to Tiago and Veríssimo (2013), the three occupy ~37% of the entire community population of CdV aquifer. On the other hand, methanogenic Archaea have not been detected, suggesting that microbial methanogenesis is not occurring in CdV mineral waters, reinforcing the results of the isotopic gas analyses (Etiope et al., 2013b). The geochemical features of CdV mineral waters prompted the hypothesis that hydrogen could be important for microbes in this geological setting. Additionally, since hydrogen sulfide has been detected in CdV mineral waters, a sulfate reducer, which can convert hydrogen to hydrogen sulfide coupled with the sulfate reduction, also needs to be investigated to identify the microbial factors that related to the paucity of H_2 in this system.

The geochemistry and biology of present-day serpentinization sites may be valuable for astrobiology because it presents an opportunity for investigating the potential geochemical and metabolic processes that had occurred on the early Earth and Mars.

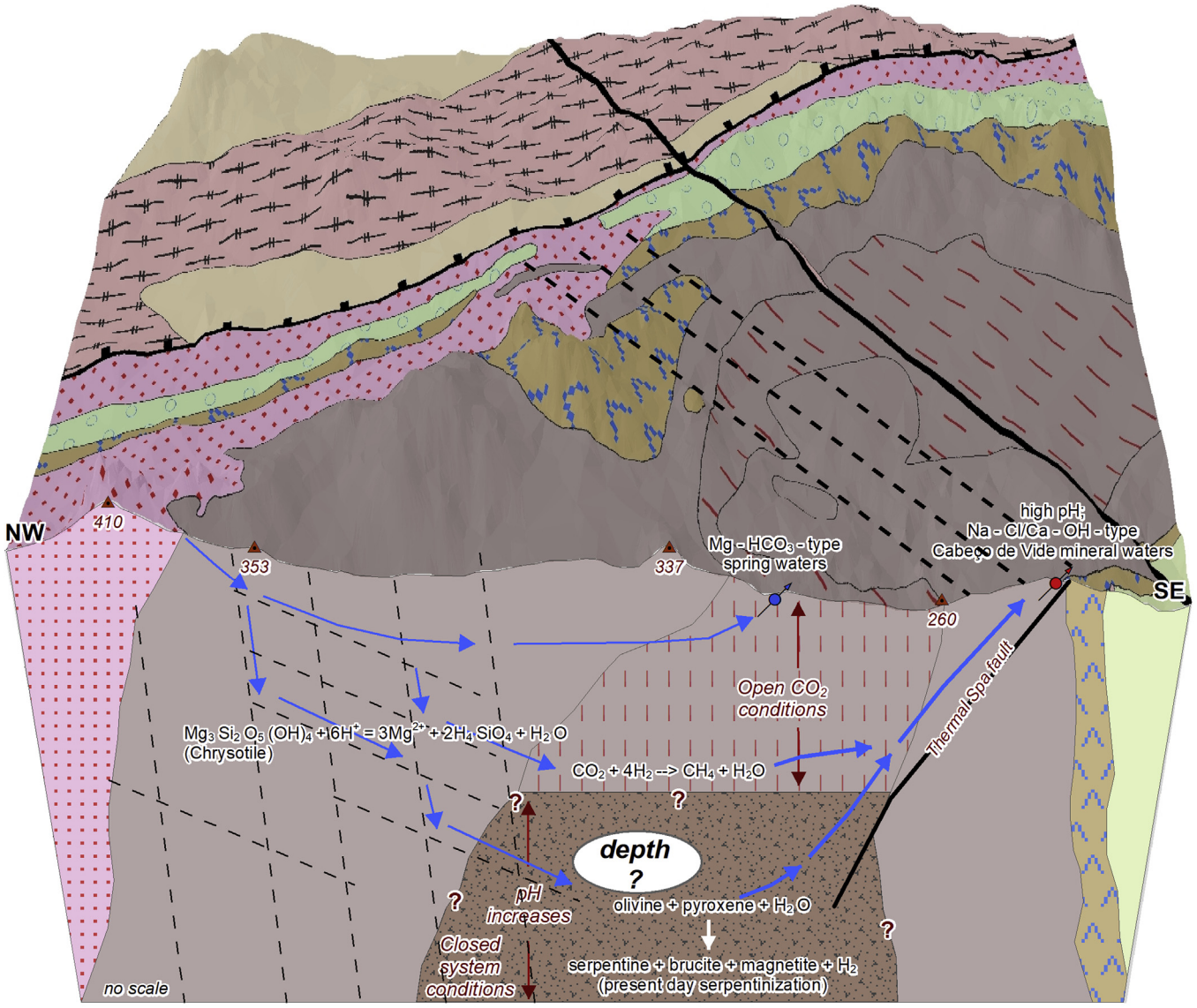

Fig. 10. Conceptual circulation model of CdV thermomineral water system (adapted from Marques et al., 2008, 2018). For detailed geological information see Fig. 1.

4. Conclusion

Combining water hydrogeology and chemistry, gas-geochemistry (molecular, isotopic, isotopologue compositions and CH_4 concentration in soil-air), microbiological and geological data, the following conceptual model can be proposed (Fig. 10):

(a) CdV hyperalkaline mineral water originates by the deep infiltration of part of the Mg-HCO_3-type waters, through major rocks discontinuities (mainly fractures), which evolve to the CdV Na-Cl/Ca-OH-type waters produced, under closed CO_2 conditions, due to water-peridotite interaction at depth. The apparent groundwater age between 3.6 ± 2.3 ka BP and 6.0 ± 2.2 ka BP, reported by Marques et al. (2008) and in this study for CdV borehole waters AC5 and AC3, respectively, supports the hypothesis that CdV mineral waters are related to deep paths (≈1 km deep, according to Pinto et al., 2004), promoting present-day serpentinization. Shallow aquifers may be episodically "contaminated" by the deeper hyperalkaline water.

(b) Methane occurs exclusively in hyperalkaline (pH > 9) waters, as documented in other serpentinization sites (e.g., Etiope et al., 2013b). Methane is likely produced abiotically at relatively low temperatures (likely < 100 °C), as suggested by isotopologue (Young et al., 2017), geological and heat flow data. If methane is produced by a catalysed abiotic synthesis such as the Sabatier reaction, as considered in a wide literature (e.g. Etiope and Sherwood Lollar, 2013), the reaction should have occurred within rocks hosting appropriate minerals, capable of acting as low temperature catalysts. In ultramafic rock systems such catalysts may occur only in chromium and PGM (e.g., ruthenium) rich rocks. Such rocks do exist at depth in the Alter-do-Chão massif. In these rocks, therefore, H_2 produced by peridotite serpentinization may have reacted in gas-phase with CO_2, likely derived by sedimentary rocks surrounding the peridotite massif. Methane may then migrate towards permeable "reservoir" rock, where it enters mineral waters that seep to the surface along faults.

(c) Microbial activity at CdV mineral waters does not seem to contribute to CH_4 production (or consumption), but might contribute to H_2 consumption, explaining the low H_2 activity in the mineral waters. Clones retrieved from the hyperalkaline aquifer (borehole AC3) were closely related to isolates belonging to the genus '*Serpentinomonas*', which are known to oxidize hydrogen (Tiago and Veríssimo, 2013; Suzuki et al., 2014; Miller et al., 2016).

(d) The tectonic contact between sedimentary and ultramafic rocks

plays a fundamental role in the mineral water and gas ascent from the reservoir to the surface. The discharge zone of the CdV mineral waters is controlled by a major, locally oriented, N-S trending faults crossing or surrounding the Alter-do-Chão peridotites, providing pathways for the upward migration of water and gas.

Combining a wide set of geological and geochemical data, we have developed a conceptual model that can explain the origin and migration of the several fluids related to serpentinization of ultramafic rocks in the CdV area (Fig. 10). This model makes the connection between geology, geochemistry and microbiology of serpentinized systems more clear. The model is generally valid for other continental serpentinization sites where hyperalkaline springs and abiotic methane have been documented. Specifically, (a) the meteoric origin of the water, (b) the low temperature (< 150 °C) and dominantly abiotic origin of the gas, (c) the fact that the fluid emissions occur at the boundary of the ultramafic units and in contact with sedimentary or metamorphic (C-bearing) rocks, are all common factors of continental gas-water bearing serpentinization sites.

Future work may focus on key mineralogical factors, primarily the presence and abundance in the deep rocks of minerals that can act as catalysts of low temperature abiotic CH_4 production (e.g., PGE (ruthenium), and microbiological questions.

Acknowledgments

This study was supported by FCT/MEC (PIDDAC) funds under the scope of the Project PTDC/AAG-MAA/2891/2012, CERENA/IST acknowledges the FCT (the Portuguese Science and Technology Foundation) support through the UID/ECI/04028/2013 Project and C^{2}TN/IST author gratefully acknowledge the FCT support through the UID/Multi/04349/2013. The study on gas origin and emission, performed by INGV, was supported by the Deep Carbon Observatory – Deep Energy community. Work performed at the Jet Propulsion Laboratory, California Institute of Technology, was done under contract with NASA and funded by the NASA Astrobiology Institute (grants 08-NAI5-0021 and 13-13NAI7_2-0024). The authors would like to thank Benjamin Tutolo and an anonymous reviewer for their comments and suggestions in order to improve a previous draft of the manuscript. The authors also would like to thank José Teixeira and Helder Chaminé for redrawing Figs. 1 and 12. The authors also would like to thank L. Rocha, Technical Director of Cabeço de Vide thermal spa, for his support during field work campaigns. Special thanks to the Junta de Freguesia of Cabeço de Vide for all the logistical support during this study. No competing financial interests exist.

Appendix A. Supplementary data

Supplementary data related to this article can be found at https://doi.org/10.1016/j.apgeochem.2018.07.011.

References

Aggarwal, P.K., Araguas-Araguas, L., Choudhry, M., van Duren, M., Froehlich, K., 2014. Lower groundwater ^{14}C age by atmospheric CO_2 uptake during sampling and analysis. Ground Water 52, 20–24.

Altschul, S.F., Gish, W., Miller, W., Myers, E.W., Lipman, D.J., 1990. Basic local alignment search tool. J. Mol. Biol. 215, 403–410.

Arnold, E.G., Cleresci, L.S., Andrew, D.E., 1992. Standard Methods for the Examination of Water and Wastewater, eighteenth ed. Published jointly by the American Public Health Association, and Water Environment Federation, Washington, D.C.

Barnes, I., O'Neil, J.R., 1969. The relationship between fluids in some fresh alpine-type ultramafics and possible modern serpentinization, Western United States. Geol. Soc. Am. Bull. 80, 1947–1960.

Barnes, I., LaMarche Jr., V.C., Himmelberg, G.R., 1967. Geochemical evidence of present-day serpentinization. Science 56, 830–832.

Barnes, I., Rapp, J.B., O'Neil, J.R., Sheppard, R.A., Gude, A.J., 1972. Metamorphic assemblages and the direction of flow of metamorphic fluids in four instances of serpentinization. Contrib. Mineral. Petrol. 35, 263–276.

Bowen, G.J., Wilkinson, B., 2002. Spatial distribution of $\delta^{18}O$ in meteoric precipitation. Geology 30, 315–318.

Brazelton, W.J., Nelson, B., Schrenk, M.O., 2012. Metagenomic evidence for H_2 oxidation and H_2 production by serpentinite-hosted subsurface microbial communities. Front. Microbiol. 2, 268. https://doi.org/10.3389/fmicb.2011.00268.

Brazelton, W.J., Morrill, P.L., Szponar, N., Schrenk, M.O., 2013. Bacterial communities associated with subsurface geochemical processes in continental serpentinite springs. Appl. Environ. Microbiol. 79, 3906–3916.

Bruni, J., Canepa, M., Cipolli, F., Marini, L., Ottonello, G., Vetuschi Zuccolini, M., 2002. Irreversible water-rock mass transfer accompanying the generation of the neutral, Mg–HCO_3 and high-pH, Ca–OH spring waters of the Genova province, Italy. Appl. Geochem. 17, 455–474.

Carneiro, A., 2014. Lugares, tempos e pessoas: povoamento rural romano no Alto Alentejo, vol. IIhttps://doi.org/10.14195/978-989-26-0833-4. Imprensa da Universidade de Coimbra (in Portuguese).

Carreira, P.M., Araújo, M.F., Nunes, D., 2005. Isotopic Composition from Rain and Water Vapour Samples from Lisbon Region: Characterization of Monthly and Daily Events. International Atomic Energy Agency publications, Vienna Final Report of a co-ordinated research project 2000-2004 "Isotopic Composition of Precipitation in the Mediterranean Basin in Relation to Air Circulation Patterns and Climate". IAEA –TEC-DOC- 1453: 141–155.

Carreira, P.M., Nunes, D., Valério, P., Araujo, M.F., 2007. An 15-year record of seasonal variation in the isotopic composition of precipitation water over continental Portugal. In: Gomes, M.E.P., Alencoão, A.M. (Eds.), XV Semana de Geoquímica e VI Congresso Ibérico de Geoquímica. UTAD, Vila Real, pp. 434–437 ISBN 987-972-669-806-7.

Cavaco, A., 1983. Relatório Final - Estudo hidrogeológico das nascentes minerais de Cabeço de Vide. Construção das captações. Furo AC3. Obra nº1730: 7 pp. (in Portuguese).

Cavaco, A., 1997. Execução de Furos de Pesquisa e Eventual captação de Água Mineral em Cabeço de Vide. Relatório Final. Refa 97020. Obra nº2829. Junta de Freguesia de Cabeço de Vide: 5 pp. (in Portuguese).

Chavagnac, V., Monnin, C., Ceuleneer, G., Boulart, C., Hoareau, G., 2013. Characterization of hyperalkaline fluids produced by low-temperature serpentinization of mantle peridotites in the Oman and Ligurian ophiolites: hyperalkaline Waters in Oman and Liguria. G-cubed 14, 2496–2522.

Cipolli, F., Gambardella, B., Marini, L., Ottonello, G., Vetuschi Zuccolini, M., 2004. Geochemistry of high-pH waters from serpentinites of the Gruppo di Voltri (Genova, Italy) and reaction path modeling of CO2 sequestration in serpentinite aquifers. Appl. Geochem. 19, 787–802.

Costa, I.R., Barriga, F., Mata, J., Munhá, J.M., 1993. Rodingitization and serpentinization processes in alter do Chão massif (NE alentejo). Mem. Mus. Lab. Min. Geol. Fac. Ciênc. Univ. Porto 3, 27–31.

Craig, H., 1961. Isotopic variations in meteoric waters. Science 133, 1703–1704.

Dallmeyer, R.D., Quesada, C., 1992. Cadomian *vs.* Variscan evolution of the Ossa-Morena zone (SW Iberia): field and $^{40}Ar/^{39}Ar$ mineral age constraints. Tectonophysics 216, 339–364.

Dias, P.A., Leal Gomes, C., Castelo Branco, J.M., Pinto, Z., 2006. Paragenetic positioning of PGE in mafic and ultramafic rocks of Cabeço de Vide – Alter do Chão Igneous Complex. In: VII Congresso Nacional de Geologia (eds. Sociedade Geológica de Portugal). Estremoz, Portugal, pp. 1007–1010.

Edgar, R.C., 2004. MUSCLE: multiple sequence alignment with high accuracy and high throughput. Nucleic Acids Res. 32, 1792–1797.

Etiope, G., 1997. Evaluation of a micro-gas chromatographic technique for environmental analyses of CO_2 and C_1-C_6 alkanes. J. Chromatogr. A 775, 243–249.

Etiope, G., 2015. Natural Gas Seepage. The Earth's Hydrocarbon Degassing. Springer, Switzerland.

Etiope, G., 2017a. Abiotic methane in continental serpentinization sites: an overview. Procedia Earth Plan. Sci. 17, 9–12.

Etiope, G., 2017b. Abiotic CH_4 in ultramafic rocks: follow the Sabatier reaction rules. In: Goldschmidt 2017 Abstract, Paris.

Etiope, G., Ionescu, A., 2015. Low-temperature catalytic CO_2 hydrogenation with geological quantities of ruthenium: a possible abiotic CH_4 source in chromitite-rich serpentinized rocks. Geofluids 15, 438–452.

Etiope, G., Schoell, M., 2014. Abiotic gas: atypical but not rare. Elements 10, 291–296.

Etiope, G., Sherwood Lollar, B., 2013. Abiotic methane on Earth. Rev. Geophys. 51, 276–299.

Etiope, G., Schoell, M., Hosgormez, H., 2011. Abiotic methane flux from the Chimaera seep and Tekirova ophiolites (Turkey): understanding gas exhalation from low temperature serpentinization and implications for Mars. Earth Planet Sci. Lett. 310, 96–104.

Etiope, G., Tsikouras, B., Kordella, S., Ifandi, E., Christodoulou, D., Papatheodorou, G., 2013a. Methane flux and origin in the Othrys ophiolite hyperalkaline springs, Greece. Chem. Geol. 347, 161–174.

Etiope, G., Vance, S., Christensen, L.E., Marques, J.M., Ribeiro da Costa, I., 2013b. Methane in serpentinized ultramafic rocks in mainland Portugal. Mar. Petrol. Geol. 45, 12–16.

Etiope, G., Judas, J., Whiticar, M.J., 2015. Occurrence of abiotic methane in the eastern United Arab Emirates ophiolite aquifer. Arab. J. Geosci. 8, 11345–11348.

Etiope, G., Vadillo, I., Whiticar, M.J., Marques, J.M., Carreira, P.M., Tiago, I., Benavente, J., Jimenez, P., Urresti, B., 2016. Abiotic methane seepage in the Ronda peridotite massif, southern Spain. Appl. Geochem. 66, 101–113.

Etiope, G., Samardžić, N., Grassa, F., Hrvatović, H., Miošić, N., Skopljak, F., 2017. Methane and hydrogen in hyperalkaline groundwaters of the serpentinized Dinaride ophiolite belt, Bosnia and Herzegovina. Appl. Geochem. 84, 286–296.

Etiope, G., Ifandi, E., Nazzari, M., Procesi, M., Tsikouras, B., Ventura, G., Steele, A., Tardini, R., Szatmari, P., 2018. Widespread abiotic methane in chromitites. Sci. Rep. 8, 8728,. https://doi.org/10.1038/s41598-018-27082-0.
Fonseca, P., Ribeiro, A., 1993. Tectonics of the Beja-Acebuches ophiolite: a major suture in the Iberian Variscan foldbelt. Geol. Rundsch. 82, 440–447.
Geyh, M.A., 2000. An overview of ^{14}C analysis in the study of groundwater. Radiocarbon 42 (1), 99–114.
Geyh, M.A., Kunzl, R., 1981. Methane in groundwater and its effect on ^{14}C groundwater dating. J. Hydrol. 52, 355–358.
Gonfiantini, R., Zuppi, G.M., 2003. Carbon isotopic exchange rate of DIC in karst groundwater. Chem. Geol. 197, 319–336.
Gonçalves, F., 1973. Carta Geológica de Portugal à escala 1:50000 e notícia explicativa para a folha 32-B Portalegre. Serv. Geol. Port. 1–45 Lisboa (in Portuguese).
Gultekin, F., Hatipoglu, E., Ersoy, A.F., 2011. Hydrogeochemistry, environmental isotopes and the origin of the Hamamayagi-Ladik thermal spring (Samsun, Turkey). Environ. Earth Sci. 62 (7), 1351–1360.
Hem, J.D., 1970. Study and Interpretation of the Chemical Characteristics of Natural Water, second ed.s. Geological Survey Water. United States Department of the Interior.
Holm, N.G., Dumont, M., Ivarsson, M., Konn, C., 2006. Alkaline fluid circulation in ultramafic rocks and formation of nucleotide constituents: a hypothesis. Geochem. Trans. 7 (7). https://doi.org/10.1186/1467-4866-7-7.
Horibe, Y., Craig, H., 1995. D/H fractionation in the system methane-hydrogen-water. Geochem. Cosmochim. Acta 59 (24), 5209–5217.
IAEA [International Atomic Energy Agency], 1976. Procedure and Technique Critique for Tritium Enrichment by Electrolysis at IAEA Laboratory. Technical Procedure 19. International Atomic Energy Agency, Vienna, Austria.
IAEA [International Atomic Energy Agency], 2009. Laser Spectroscopic Analysis of Liquid Water Samples for Stable Hydrogen and Oxygen Isotopes. Training Course Series 35 (IAEA-tcs-35). International Atomic Energy Agency, Vienna, Austria.
IGM [Instituto Geológico e Mineiro], 1998. Recursos geotérmicos em Portugal continental: baixa entalpia. in Portuguese). http://www.lneg.pt/CienciaParaTodos/edicoes_online/diversos/rec_geotermicos/texto.
Kumar, S., Stecher, G., Tamura, K., 2016. MEGA7: molecular evolutionary genetics analysis version 7.0 for bigger datasets. Mol. Biol. Evol. 33, 1870–1874.
Lane, D.J., 1991. 16S/23S rRNA sequencing. In: Stackenbrandt, E., Goodfellow, M. (Eds.), Nucleic Acid Techniques in Bacterial Systematic. John Wiley, Chichester, pp. 115–175.
Malvoisin, B., Brunet, F., 2014. Water diffusion-transport in a synthetic dunite: consequences for oceanic peridotite serpentinization. Earth Planet Sci. Lett. 403, 263–272.
Marques, J.M., Carreira, P.M., Carvalho, M.R., Matias, M.J., Goff, F.E., Basto, M.J., Graça, R.C., Aires-Barros, L., Rocha, L., 2008. Origins of high pH mineral waters from ultramafic rocks, Central Portugal. Appl. Geochem. 23, 3278–3289.
Marques, J.M., Carreira, P.M., Neves, O., Espinha Marques, J., Teixeira, J., 2018. Revision of the hydrogeological conceptual models of two Portuguese thermomineral water systems: similarities and differences. Sustain. Water Res. Manag. https://doi.org/10.1007/s40899-018-0218-8.
Mata, J., Munhá, J., 1985. Geochemistry of mafic metavolcanic rocks from the Estremoz region (South-Central Portugal). Com. Serv. Geol. Port. 71, 175–185.
McCollom, T.M., 2007. Geochemical constrains on sources of metabolic energy for chemolithoautotrophy in ultramafic-hosted deep-sea hydrothermal systems. Astrobiology 7, 933–950.
McCollom, T.M., Bach, W., 2009. Thermodynamic constrains on hydrogen generation during serpentinization of ultramafic rocks. Geochem. Cosmochim. Acta 73, 856–875.
McCollom, T.M., Seewald, J.S., 2013. Serpentinites, hydrogen, and life. Elements 9, 129–134.
Miller, A.Z., Suzuki, S., Rocha, C., Marques, J.M., 2016. Terrestrial serpentinization: new insights into the adaptation and evolution of microbial life on the early Earth. In: Book of Abstracts of the 16th EANA Astrobiology Conference, Part B – B87.
Monnin, C., Chavagnac, V., Boulart, C., Ménez, B., Gérard, M., Gérard, E., Quéméneur, M., Erauso, G., Postec, A., Guentas-Dombrowski, L., Payri, C., Pelletier, B., 2014. The low temperature hyperalkaline hydrothermal system of the Prony bay (New Caledonia). Biogeosci. Discuss. 11, 6221–6267.
Morrill, P.L., Kuenen, J.G., Johnson, O.J., Suzuki, S., Rietze, A., Sessions, A.L., Fogel, M.L., Nealson, K.H., 2013. Geochemistry and geobiology of a present-day serpentinization site in California: the Cedars. Geochem. Cosmochim. Acta 109, 222–240.
Mottl, M.J., Komor, S.C., Fryer, P., Moyer, C.L., 2003. Deep-slab fluids fuel extremophilic Archaea on a mariana forearc serpentinite mud volcano: ocean drilling program leg 195. G-cubed 4 (11). https://doi.org/10.1029/2003GC000588.
Oehler, D.Z., Etiope, G., 2017. Methane seepage on Mars: where to look and why. Astrobiology. https://doi.org/10.1089/ast.2017.1657.
Pinto, Z., Pañeda, A., Castelo Branco, J.M., 2004. Área de Campo Maior. Relatório inédito de prospecção e pesquisa (2º semestre de 2004) da Rio Narcea Gold Mines S. A., 15 p. + anexos. in Portuguese).
Proskurowski, G., Lilley, M.D., Seewald, J.S., Früh-Green, G.L., Olson, E.J., Lupton, J.E., Sylva, S.P., Kelley, D.S., 2008. Abiogenic hydrocarbon production at Lost City hydrothermal field. Science 319, 604–607.
Rocha, L., 2006. Proposta para a definição do perímetro de proteção das Termas de Cabeço de Vide. Concessão HM-36. Junta de Freguesia de Cabeço de Vide. pp. 1–44 (in Portuguese).
Rozanski, K., Araguás-Araguás, L., Gonfiantini, R., 1993. Isotopic patterns in modern global precipitation. In: In: Swart, P.K., Lohmann, K.C., McKenzie, J., Savin, S. (Eds.), Climate Change in Continental Isotopic Records, vol. 78. American Geophysical Union, Geophys. Monogr. Ser, pp. 1–36.
Russell, M.J., Hall, A.J., Martin, W., 2010. Serpentinization as a source of energy at the origin of life. Geobiology 8, 355–437.
Russell, M.J., Barge, L.M., Bhartia, R., Bocanegra, D., Bracher, P.J., Branscomb, E., Kidd, R., McGlynn, S., Meier, D.H., Nitschke, W., Shibuya, T., Vance, S., White, L., Kanik, I., 2014. The drive to life on wet and icy worlds. Astrobiology 14 (4), 308–343.
Salem, O., Visser, J.M., Dray, M., Gonfiantini, R., 1980. Groundwater flow patterns in the western Libyan Arab Jamahiriya evaluated from isotopic data. In: I.A.E.A. (Ed.), Arid-zone Hydrology: Investigation with Isotope Techniques. IAEA, Vienna, pp. 165–179.
Sanchez-Murillo, R., Gazel, E., Schwarzenbach, E., Crespo-Medina, M., Schrenk, M.O., Boll, J., Gill, B.C., 2014. Geochemical evidence for active tropical serpentinization in the Santa Elena Ophiolite, Costa Rica: an analog of a humid early Earth? G-cubed 15, 1783–1800.
Schloss, P.D., Handelsman, J., 2005. Introducing species richness DOTUR, a computer program for defining operational taxonomic units and estimating. Appl. Environ. Microbiol. 71, 1501–1506.
Schrenk, M.O., Brazelton, W.J., Lang, S.Q., 2013. Serpentinization, carbon, and deep life. Rev. Mineral. Geochem. 75, 575–606.
Schulte, M., Blake, D., Hoehler, T., McCollom, T., 2006. Serpentinization and its implications for life on the early Earth and Mars. Astrobiology 6, 364–376.
Snaidr, J., Amann, R., Huber, I., Ludwig, W., Schleifer, K.-H., 1997. Phylogenetic analysis and in situ identification of bacteria in activated sludge. Appl. Environ. Microbiol. 63, 2884–2896.
Suda, K., Ueno, Y., Yoshizaki, M., Nakamura, H., Kurokawa, K., Nishiyama, E., Yoshino, K., Hongoh, Y., Kawachi, K., Omori, S., Yamada, K., Yoshida, N., Maruyama, S., 2014. Origin of methane in serpentinite-hosted hydrothermal systems: the CH_4–H_2–H_2O hydrogen isotope systematics of the Hakuba Happo hot spring. Earth Planet Sci. Lett. 386, 112–125.
Suzuki, S., Ishii, S., Wu, A., Cheung, A., Tenney, A., Wanger, G., Kuenen, J.G., Nealson, K.H., 2013. Microbial diversity in the Cedars, an ultrabasic, ultrareducing, and low salinity serpentinizing ecosystem. www.pnas.org/cgi/doi/10.1073/pnas.1302426110.
Suzuki, S., Kuenen, J.G., Schipper, K., van der Velde, S., Ishii, S., Wu, A., Sorokin, D.Y., Tenney, A., Meng, X., Morrill, P.L., Kamagata, Y., Muyzer, G., Nealson, K.H., 2014. Physiological and genomic features of highly alkaliphilic hydrogen-utilizing Betaproteobacteria from a continental serpentinizing site. Nat. Commun. https://doi.org/10.1038/ncomms4900.
Suzuki, S., Ishii, S., Hoshino, T., Rietze, A., Tenney, A., Morrill, P.L., Inagaki, F., Kuenen, J.G., Nealson, K.H., 2017. Unusual metabolic diversity of hyperalkaliphilic microbial communities associated with subterranean serpentinization at the Cedars. ISME J. 11, 2584–2598.
Terzer, S., Wassenaar, L.I., Araguás-Araguás, L., Aggarwal, P.K., 2013. Global isoscapes for $\delta^{18}O$ and $\delta^{2}H$ in precipitation: improved prediction using regionalized climatic regression models. Hydrol. Earth Syst. Sci. 17, 4713–4728.
Tiago, I., Veríssimo, A., 2013. Microbial and functional diversity of a subterrestrial high pH groundwater associated to serpentinization. Environ. Microbiol. 15 (6), 1687–1706.
Vacquand, C., Deville, E., Beaumont, V., Guyot, F., Sissmann, O., Pillot, D., Arcilla, C., Prinzhofer, A., 2018. Reduced gas seepages in ophiolitic complexes: evidences for multiple origins of the H_2-CH_4-N_2 gas mixtures. Geochem. Cosmochim. Acta 233, 437–461.
Vance, S., Harnmeijer, J., Kimura, J., Hussmann, H., de Martin, B., Brown, J.M., 2007. Hydrothermal systems in small ocean planets. Astrobiology 7 (6), 987–1005.
Vance, S., Hand, K., Pappalardo, R., 2016. Geophysical controls of chemical disequilibria in Europa. Geophys. Res. Lett. https://doi.org/10.1002/2016GL068547.
Vogel, J.S., Southon, J.R., Nelson, D.E., Brown, T.A., 1984. Performance of catalyticaly condensed carbon for use in acelerator mass spectrometry. In: In: Wolfi, W., Polach, H.A., Anderson, H.H. (Eds.), Procedings of the 3rd International Symposium on Acelerator Mass Spectrometry B5. pp. 289–293 Nuclear Instruments and Methods in Physics Research.
Voronov, A.N., Vinograd, N.A., 2009. The Lower-Kotlin aquifer as a source of mineral therapeutic waters for St. Petersburg. Environ. Earth Sci. 59 (1), 15–20.
Wang, D.T., Reeves, E.P., McDermott, J.M., Seewald, J.S., Ono, S., 2018. Clumped isotopologue constraints on the origin of methane at seafloor hot springs. Geochem. Cosmochim. Acta 223, 141–158.
Young, E.D., Kohl, I.E., Sherwood Lollar, B., Etiope, G., Rumble III, D., Li, S., Haghnegahdar, M.A., Schauble, E.A., McCain, K.A., Foustoukos, D.I., Sutclife, C., Warr, O., Ballentine, C.J., Onstott, T.C., Hosgormez, H., Neubeck, A., Marques, J.M., Pérez-Rodríguez, I., Rowe, A.R., LaRowe, D.E., Magnabosco, C., Yeung, L.Y., Ash, J.L., Bryndzia, L.T., 2017. The relative abundances of resolved $^{12}CH_2D_2$ and $^{13}CH_3D$ and mechanisms controlling isotopic bond ordering in abiotic and biotic methane gases. Geochem. Cosmochim. Acta 203, 235–264.